Plant Science 339 (2024) 111962

Contents lists available at ScienceDirect

Plant Science

journal homepage: www.elsevier.com/locate/plantsci

Dephosphorylation of the MAP kinases MPK6 and MPK3 fine-tunes responses to wounding and herbivory in Arabidopsis

Claire T. Hann [a], Sophia F. Ramage [a], Harshita Negi [a], Carlton J. Bequette [a,1], Paula A. Vasquez [b], Johannes W. Stratmann [a,*]

[a] Department of Biological Sciences, University of South Carolina, Columbia, SC 29208, United States
[b] Department of Mathematics, University of South Carolina, Columbia, SC 29208, United States

ARTICLE INFO

Keywords:
MAP kinase
MAPK phosphatase
Jasmonic acid
Abscisic acid
Salicylic acid
Herbivory

ABSTRACT

The Arabidopsis MAP Kinases (MAPKs) MPK6 and MPK3 and orthologs in other plants function as major stress signaling hubs. MAPKs are activated by phosphorylation and are negatively regulated by MAPK-inactivating phosphatases (MIPPs), which alter the intensity and duration of MAPK signaling via dephosphorylation. Unlike in other plant species, jasmonic acid (JA) accumulation in *Arabidopsis* is apparently not *MPK6*- and *MPK3*-dependent, so their role in JA-mediated defenses against herbivorous insects is unclear. Here we explore whether changes in MPK6/3 phosphorylation kinetics in Arabidopsis MIPP mutants lead to changes in hormone synthesis and resistance against herbivores. The MIPPs MKP1, DsPTP1, PP2C5, and AP2C1 have been implicated in responses to infection, drought, and osmotic stress, which all impinge on JA-mediated defenses. In loss-of-function mutants, we found that the four MIPPs alter wound-induced MPK6/3 phosphorylation kinetics and affect the accumulation of the defense hormones JA, abscisic acid, and salicylic acid, as compared to wild type plants (Col-0). Moreover, *MPK6/3* misregulation in MIPP or MAPK mutant plants resulted in slight changes in the resistance to *Trichoplusia ni* and *Spodoptera exigua* larvae as compared to Col-0. Our data indicate that MPK6/3 and the four MIPPs moderately contribute to wound signaling and defense against herbivorous insects in Arabidopsis.

1. Introduction

Tissue wounding by chewing herbivorous insects results in the release of alarm signals from damaged cells (damage-associated molecular patterns) or from the insects (herbivore-associated molecular patterns). As a consequence, jasmonic acid (JA) and the drought hormone abscisic acid (ABA) accumulate close to wound sites (Vos et al. 2013). Perception of alarm signals by pattern recognition receptors results in activation of MAPK cascades which regulate defense gene expression via the phosphorylation of transcription factors. Because many different stresses result in activation of the same MAPKs, they represent shared signaling hubs. This is especially the case for the two closely related Arabidopsis paralogs AtMPK6 and AtMPK3 (MPK6/3), which are activated by many biotic and abiotic stressors. AtMPK6/3 are strongly activated by mechanical wounding and have overlapping roles (Sözen et al. 2020; Ichimura et al., 2000; Rayapuram et al. 2018). Strong activation of MPK6/3 orthologs by insect feeding has been demonstrated in tobacco and tomato (Kandoth et al. 2007; Wu et al. 2007).

In plants like tobacco and tomato, MPK6 is essential for JA synthesis (Kandoth et al. 2007; Wu et al. 2007), but Arabidopsis MPK6 may function downstream of JA and negatively impact JA synthesis (Wasternack and Hause, 2013; van Verk et al. 2011; Takahashi et al. 2007). This makes the role of this essential MAPK signaling hub unclear in the context of Arabidopsis wound responses. Wounding rapidly induces JA synthesis close to the wound site (Glauser et al. 2008). Once the active JA derivative JA-isoleucine is perceived by the COI1 (CORONATINE INSENSITIVE 1) receptor, the transcription factor and master regulator MYC2 (JASMONATE INSENSITIVE 1) is derepressed and can induce the expression of JA biosynthetic genes and defense genes, generating a positive feedback loop that leads to further JA biosynthesis (Lorenzo et al., 2004). This results in the accumulation of antinutritive proteins and toxic secondary metabolites, including glucosinolates, flavonoids, and alkaloids (Guo et al. 2018; Sheard et al. 2010). In addition, MPK6/3 activity has been shown to induce transcription of the abscisic

Abbreviations: MIPP, MAPK-inactivating phosphatase; WSRT, Wilcoxon Signed Rank Test.

* Corresponding author.
E-mail address: johstrat@biol.sc.edu (J.W. Stratmann).
[1] Present address: Reynolds American Inc., Winston-Salem, NC, USA

https://doi.org/10.1016/j.plantsci.2023.111962
Received 14 August 2023; Received in revised form 24 November 2023; Accepted 12 December 2023
Available online 15 December 2023

acid (ABA) biosynthesis rate-limiting enzyme NCED3 (9-*CIS*-EPOXYCAROTENOID DIOXYGENASE 3) during development (Xing et al. 2009). NCED3 transcript is also rapidly induced in response to a loss in leaf turgor (Sussmilch et al. 2017). Loss of leaf turgor is associated with wounding events and can be detected by individual cells adjacent to a wound site (Hoermayer et al. 2020). While the link between MPK6 activity and ABA accumulation is not well described, these reports suggest that MPK6 can support wound-induced de-novo synthesis of ABA. Wounding results in ABA accumulation at the wound site (Heyer et al. 2018; Birkenmeier and Ryan, 1998), and ABA signaling supports JA-dependent signaling against chewing insects (Vos et al. 2013; Yu et al. 2021; Sözen et al. 2020; Lawrence et al. 2022). MPK6/3 are not known to play a role in SA synthesis in Arabidopsis (Zhang and Zhang, 2022), but SA may affect responses to herbivory via crosstalk with JA signaling (Nomoto et al. 2021). These hormones repress one another at both the hormone synthesis and target gene levels (Van der Does et al. 2013; Wei et al. 2014).

MAP kinases (MAPKs) play critical roles as signal transducers in responses to many biotic and abiotic stresses (Zhang and Zhang, 2022). Plant MAPKs are active when dually phosphorylated by a MAPK kinase at a threonine (T) and a tyrosine (Y) in a TE/DY phosphorylation motif within the kinase activation loop (Marshall, 1994; Ichimura et al. 2002). MAPKs are negatively regulated by MAPK inactivating phosphatases (MIPPs), also known as MAPK phosphatases (MKPs) resulting in altered phosphorylation kinetics. MIPPs inactivate MAPKs by dephosphorylation of phospho-T (serine/threonine-specific phosphatases such as members of the PP2Cs family), phospho-Y (tyrosine-specific phosphatases, PTPs), or both phospho-T and phospho-Y (dual-specificity phosphatases or DSPs). Reducing MAPK activity by MIPPs via dephosphorylation of the TE/DY motif at the right time is as important as MAPK activation by MAPK kinases.

MAPKs like Arabidopsis MPK6 and MPK3 function like hub proteins for many different forms of stress and are required for proper stress responses (Zhang and Zhang, 2022). To achieve signaling specificity MAPKs interact with MAPK kinases, which in turn are activated by MAPK kinase kinases in a dedicated MAPK cascade in specific cellular locales, mostly the cytosol and the nucleus. In addition, the timing of MAPK activation, the response amplitude, and downregulation of MAPK activity by MIPPs confer specificity to MAPK signaling leading to specific cellular responses. Through dephosphorylation of MAPKs, MIPPs may determine all three aspects of MAPK function, resulting in an input-specific pattern of MAPK kinetics (Bartels et al. 2010; Jiang et al., 2018; Schweighofer et al. 2004).

This study is focused on four MIPPs, the DSPs DsPTP1 and MKP1, and the two clade-A PP2Cs AP2C1 and PP2C5 (also known as AP2C3). Previous studies have shown that these four MIPPs can regulate MPK6/3 kinetics in responses to drought (Liu et al. 2015; Brock et al., 2010) and pathogens (Jiang et al., 2018; Anderson et al. 2011; Bartels et al. 2009; Schweighofer et al. 2007). Therefore, they may also be involved in the regulation of ABA and salicylic acid (SA) synthesis (Verma et al., 2020). SA is critical for defenses against pathogens (Ayatollahi et al. 2022). Since these two hormones indirectly regulate JA-dependent wound responses, individual MIPPs may participate in shaping the wound response. In addition, MKP1, AP2C1, and PP2C5 have been shown to physically interact with MPK6 and MPK3 (Schweighofer et al. 2007; Umbrasaite et al. 2010; Ayatollahi et al. 2022; Ulm et al. 2002).

MIPPs have been shown to change MAPK kinetics in response to mechanical wounding (Ayatollahi et al. 2022; Brock et al., 2010; Schweighofer et al. 2007) and to be wound-inducible (Winter et al. 2007), but their roles in defense against herbivores has not been studied. In this paper, we aim to clarify the role of MPK6/3 in regulating defense against chewing insects by studying *mpk6, mpk3*, *dsptp1*, *mkp1*, *ap2c1*, and *ap2c5* loss-of-function mutants. We hypothesized that given the broad involvement of MPK6/3 in regulating responses to stress, changes in MPK6/3 kinetics can impact induced defenses against insect herbivores. We found that altering MPK3/6 kinetics in MAPK or in MIPP mutants modulates wound-induced JA, ABA, and SA synthesis and responses to herbivores.

2. Materials and methods

2.1. Plants

Plants were raised on soil (Sun-Gro Professional Mix) on a 16 h light (22 °C) and 8 h dark (20 °C) long day cycle in a Percival reach-in growth chamber (Percival Scientific, Perry, IA), at 150 μ E m^{-2} s^{-1}. Plants were fertilized using MiracleGro All-Purpose Plant food (MiracleGro). Mutant lines *ap2c1* ("ap2c1–2," SALK_065126.55.00.x, Schweighofer et al. 2007) and *pp2c5* ("pp2c5–2″ in Fig. 1; SALK_109986.48.00.x; Brock et al., 2010) were a kind gift by Andrea Gust; the *dsptp1* (SALK_092811.54.50.x, Liu, R. et al. 2015) line was obtained from the Arabidopsis Stock Center (ABRC). Homozygous genotype was confirmed via PCR using the primers in Table A.1.2 (Fig. A.1.1; Appendix A.1.1). The *mkp1* line was a kind gift by Scott Peck (González Besteiro and Ulm, 2013) and confirmed phenotypically (Fig. A.1.1 D; Appendix A.1.1). The *mpk6* line (*mpk6–2*, SALK_073907) and the *mpk3* line (*mpk3–1*, SALK_151594) were obtained from ABRC, described previously (Liu and Zhang, 2004; Zhao et al. 2014), and confirmed via Western blotting. Three mutants are shown in Fig. 1, which were not included in the remaining analyses, *ap2c1–1* (SAIL_590_B11), *pp2c5–1* (SALK_015191C), and a *dsptp1/pp2c5–1* double mutant. For MAPK assays (Materials and Methods 2.2) and hormone analyses (Materials and Methods 2.3), 2.5-week-old plants were used Fig. 2.

2.2. MAPK Assays

Experiments were performed in a separate walk-in growth chamber with the same growth conditions described in Materials and Methods 2.1. Samples (genotype/time) contained n = 10 plants; on each plant, two opposite leaves received a 2 mm-wide wound at the midline of the leaf oriented perpendicular to the midvein, using a rippled forceps. Samples were collected by excising one leaf from each plant at the base of the leaf, and freezing the ten leaves simultaneously in liquid nitrogen. A maximum of 45 s elapsed between the excision of the first leaf and sample freezing. The second set of leaves was collected immediately afterwards, using the same method, and stored for hormone analysis if appropriate (Materials and Methods 2.3). Genotypes were sampled on the same day and within the same hour. Time points (15′−180′) were collected after 6 h of light exposure. Unwounded (0′) samples were collected at the same time of day from a cohort of naïve plants raised alongside treated plants.Fig. 3.

Frozen samples were pulverized by hand in a mortar under liquid nitrogen; lysis buffer (Grissett et al. 2020) was added to the mortar for sample homogenization. Twenty to thirty μg total protein was analyzed for MAPK phosphorylation by immunoblotting using anti-phospho-ERK primary antibody (phospho-p44/42 MAPK (Erk1/2; Thr202/Tyr204); D13.14.4E; Cell Signaling Technology) in 5% BSA at a 1:2000 dilution. Phosphorylated MAPK signals were detected with Goat Anti-Rabbit IgG-HRP conjugate secondary antibody (Bio-Rad) at a 1:20,000 dilution, coupled with an alkaline phosphatase substrate (Clarity Western ECL Substrate, Bio-Rad). Imaging was performed with x-ray film and/or digital imager. Scans or images were converted to JPEG format, and bands were quantified using ImageJ (NIH) (Schneider et al. 2012). Coomassie Brilliant Blue (CBB) staining was used to confirm equal protein loading before quantification (Appendix A.2). In fold comparisons, results from individual mutants were compared to Col-0 (Col-0 = 1). Significant differences were calculated using Wilcoxon Signed Rank Test (WSRT) for small data sets lacking a normal distribution. A version of the WSRT called "method of Pratt" was used; this test accounts for all control values being equal, i.e., Col-0 = 1 (Appendix B.1).

2.3. Hormone Analysis via LC-MS

For each time point, ten plants of each line were treated and sampled as described for MAPK assays (Materials and Methods 2.2). The method for extraction and analysis was adapted from Glauser et al. 2008. Samples were weighed, then pulverized by hand in a mortar under liquid nitrogen; 1 mL of isopropanol was added per 100 mg of sample weight. Samples contained 200–300 mg of tissue. 1 mL of homogenized sample was collected in a glass vial, and 10 ng d6ABA (or (+/+)− 2-cis-4--trans-Abscisic Acid-d6, ICON Isotopes), 100 ng dhJA (or (-)− 9, 10-Dihydrojasmonic acid), and 100 ng d4SA (or salicylic acid-d4) were added as internal standards to each vial. Samples were then dried under compressed nitrogen at 40 °C. 1.5 mL of an 85:15 MeOH/H2O solution was used to resuspend the dried sample. The resuspension was then allowed to pass through a SepPak Vac 100 mg C18 cartridge (Waters) that was primed once with 1 mL resuspension solution. Residual eluate was flushed using 0.5 mL of resuspension solution. Eluate was collected and redried under compressed nitrogen at 40 °C. Extract was resuspended in 300 μL of resuspension solution and hormones were quantified by HPLC-MS analysis (see below).

The amount of analyte (ng/g fresh weight) detected was calculated using area-under-the-curve (AUC) ratios (generated by HPLC-MS software) of endogenous analyte signals over an internal deuterated standard (dh-JA, d4-SA, and d6-ABA), and confirmed by establishing a standard curve for each hormone analyte. We plotted time courses of sample concentrations detected as nmol/g FW to show changes in sample concentration over time. To make comparisons between hormone levels detected in mutant samples at individual times (second columns in Figs. 4–6), we chose to report ng hormone/g FW. This was intended to facilitate comparisons with other reports. We also converted all values for all time points post-wounding to fold over corresponding Col-0 value in each replicate and pooled them for statistical analysis. Statistical analysis was performed using the WSRT due to small data set size and because data sets were not normally distributed. A version of the WSRT called "method of Pratt" was used in analyses comparing fold values (mutant vs. Col-0); in this test all control values (Col-0) are equal (= 1). In fold comparisons, individual mutant results were divided by the Col-0 result (or the 0′ result) for that replicate, then compared to 1, reporting relative proportions of accumulated hormone (Appendix B.2).

HPLC-MS analyses were performed on a Thermo Vanquish HPLC system coupled with a Thermo Q-Exactive HF-X quadrupole/orbitrap high resolution mass spectrometer operated in negative ion mode using the IonMax II electrospray source. The chromatographic separation was carried out on a Waters Xbridge BEH C18 column (2.1 mm X 100 mm, 3.5 μm) with the following solvent system: solvent A: Water with 0.1% formic acid; solvent B: acetonitrile with 0.1% formic acid. A gradient elution was performed at a flow rate of 0.2 mL/min at a column temperature of 40 °C under these conditions; 5% B 0–2 min; 20% B at 7 min; 30% B at 20 min; and 95% B at 28 min and holding to 35 min There was a 5 min re-equilibration time to return to initial conditions. The mass scanning utilized high resolution parallel reaction monitoring (HRPRM) with: Resolution, 30,000; AGC target, 1E6; Maximum IT, 200 ms; Isolation window, 1.1 *m/z* and NCE, 35. The M-H ion for each analyte was used in the inclusion list for HRPRM. Fragment ions monitored were: SA, 93.0 *m/z*; d4 SA, 97.1 *m/z*; JA, 59.0 *m/z*; dhJA, 59.0 *m/z*; ABA, 204.1 *m/z*; d6 ABA, 225.2 *m/z*.

2.4. Larval growth assays

Experiments were performed under growth conditions described above (Materials and Methods 2.1). For *Trichoplusia ni* assays, *T. ni* eggs (Benzon Research, Carlisle, PA) were hatched at 27 °C on Col-0 plants. 1–2 day-old-larvae were individually transferred into tented plant boxes to isolate the larvae. Each box (3″x4″) contained 8 2-week-old plants of the same genotype (no-choice experiment). Larvae were allowed to feed on the same plants until pupation and were weighed on day 10, 12 and 14. Pupation was expected on day 16, with pre-pupation weight loss expected on days 15–16. Statistical significance was calculated using WSRT due to data sets for some lines not following a normal distribution. (Appendix B.3).

For *Spodoptera exigua* assays, plants were raised on a 16 h light (23 °C) / 8 h dark (22 °C) diurnal cycle in 24 cm × 44 cm x 18 cm transparent boxes. Boxes contained soil to a height of 10 cm, and plants were planted in a 13 × 20 plants grid arrangement to create a lawn. Boxes were secured with plastic wrap to prevent larval escape. Temperature was raised from the standard 22 °C/20 °C day/night program to a 23 °C day/ 22 °C night program to ensure safer larval growth. Larvae were hatched on artificial medium (Benzon Research, Carlisle, PA) and raised for one week at 28 °C before transfer. This was necessary due to the higher temperature requirements for *S. exigua* larval development; neonate larvae did not thrive at standard temperatures used for Arabidopsis growth but could continue development with slightly raised temperatures after the first instar. Larvae (n = 12) were weighed, then transferred to each box, and allowed to feed for two days, then weighed each subsequent day until pupation while continuing to feed on the same plants. Statistical significance was calculated using WSRT (Appendix B.4).

3. Results

3.1. Wound-induced MAPK phosphorylation kinetics are altered in MIPP loss-of-function mutants

Since each MIPP shows stress-specific MAPK binding specificity and gene expression, we tested whether knockout of the MIPP genes *AP2C1*, *PP2C5*, *DsPTP1*, and *MKP1* in T-DNA insertional mutant plants (Fig. A.1.1) would result in distinct effects on wound-induced MPK6/3 phosphorylation kinetics in Arabidopsis (Fig. 1). We included the *mpk6* and *mpk3* loss-of-function mutants. All mutants were in the Col-0 background and were analyzed for MPK6/3 phosphorylation by immunoblotting before (0 min) and after wounding (15, 30, 60, and 90 min) with a rippled forceps. We also detected phosphorylation of another MAPK, presumably MPK4 (Fig. 1). In addition, we analyzed the insertional mutant lines *ap2c1–1* and *pp2c5–1* as well as the double mutant *dsptp1/pp2c5–1*. We measured a significant amount of the respective transcripts in these mutants and therefore we did not include them in further analyses. As null mutants, *mpk6* and *mpk3* show complete loss of MPK6 and MPK3 phosphorylation (Liu and Zhang 2004; Zhao et al. 2014).

Phosphorylation signals on blots were quantified, and, for each time point, fold values in mutant lines over Col-0 (= 1 fold) were determined for MPK6 and MPK3 phosphorylation. For MPK6, higher phosphorylation was found at 60 min in the *ap2c1* line (Fig. 2 *C*) and at 90 min in the *ap2c1, pp2c5,* and *mpk3* mutant lines (Fig. 2 *D*). We found that statistical significance for earlier time points would have required more replicates (Wilcoxon Signed Rank test; Appendix B.1.1). For an alternative assessment, we plotted a heat map of median values from each mutant at each time point (Fig. 2 *E*). Most mutant lines showed elevated MPK6 and or MPK3 phosphorylation at one or more time points. However, at 30 min, no mutant showed significant MPK6 phosphorylation above Col-0. The *ap2c1* mutant had reduced MPK6 phosphorylation early in the time course but showed increased MPK6 phosphorylation late in the time course. The *dsptp1* mutant showed strongly elevated MPK6 phosphorylation early in the time course only. The *mkp1* mutant had reduced MPK6 phosphorylation throughout the time course. The *pp2c5* mutant showed increased MPK6 phosphorylation throughout the time course, as did the *mpk3* mutant; the *mpk3* mutant showed the strongest MPK6 phosphorylation signal. This shows that different MIPPs affect MAPK phosphorylation at different times after wounding as shown in Fig. 2 F.

In Col-0, MPK6 and MPK3 show similar phosphorylation kinetics. MPK3 kinetics were impacted in MIPP loss-of-function mutants at the 15- and 60-min time points. The *ap2c1* mutant showed elevated activity

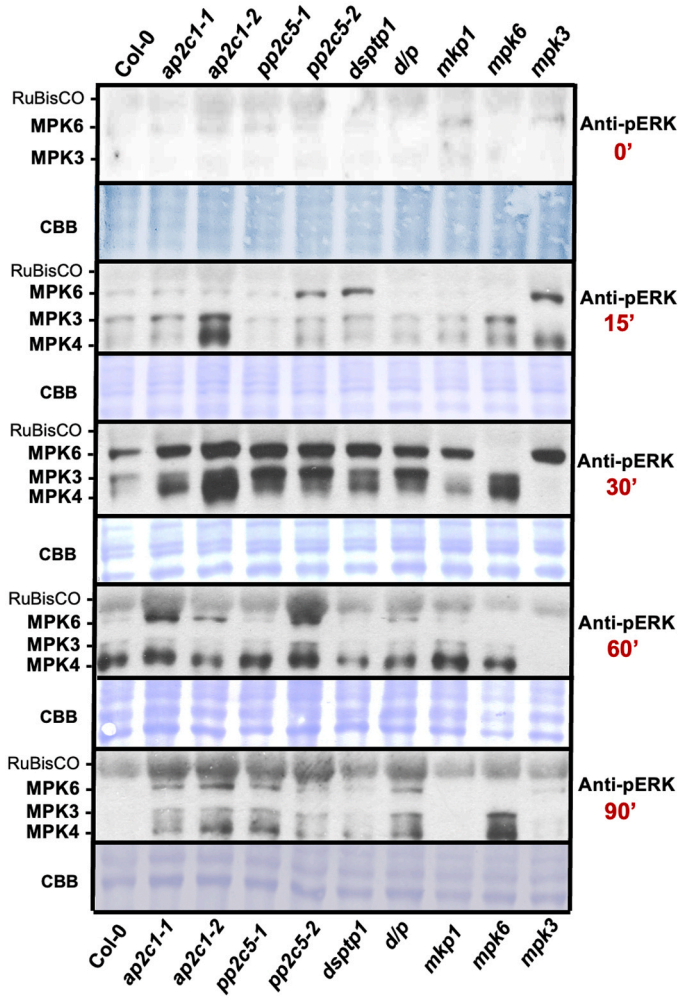

Fig. 1. Wound-induced MAPK phosphorylation kinetics are regulated by MIPPs. 3-week-old Col-0 and mutant plants were wounded with forceps and analyzed by immunoblotting with an anti-pERK antibody that recognizes MAPKs dually phosphorylated in the TEY phosphorylation motif. A representative experiment is shown. All experiments are shown in Figs. A.2.1 – A.2.5. MPK6 (47 kDa), MPK3 (43 kDa), and MPK4 (39 kDa) positions are indicated. The diffuse band above MPK6 is due to unspecific binding of antibodies to a prominent protein, presumably RuBisCO. *d/p = dsptp1/pp2c5–1* double mutant - not further analyzed; other mutants are explained in the text. CBB-stained blots show protein loading. Exposure times for each timepoint varied to accommodate for different signal intensities. All signals in mutants are compared to Col-0 (lane 1), and not to signals from other time points.

at 15 min, indicating an early negative effect of AP2C1 on MPK3 kinetics. The *pp2c5* mutant showed lower MPK3 phosphorylation at 15 min and elevated phosphorylation at 60 min, indicating late negative regulation of MPK3 kinetics (Fig. 3 A and C). The *mkp1* mutant also showed elevated phosphorylation of MPK3 at 60 min (5/5 experiments, Fig. 3 C). The *mpk6* mutant showed the strongest MPK3 phosphorylation signal (Fig. 3 E) (Appendix B.1.2).

In the *mpk6* mutants, we found elevated wound-induced MPK3 phosphorylation, and in *mpk3* mutants elevated wound-induced MPK6 phosphorylation (Fig. 2 and Fig. 3) in most experiments at 15, 60, and 90 min. This indicates that the two MAPKs mutually regulate each other via a mechanism yet to be determined.

3.2. Defense hormone analysis

To test whether changes in wound-induced MAPK phosphorylation kinetics correlate with changes in levels of defense hormones, we measured the hormones jasmonic acid (JA), salicylic acid (SA), and ABA post wounding. One leaf per plant was wounded as described for Fig. 1. We then collected and extracted each sample (10 plants) for HPLC-MS analysis. Hormone levels were calculated as ng/g fresh weight (FW) and converted to nmol/g FW for time courses. We also expressed all values for all times post wounding as fold over the corresponding Col-0 value and pooled them for statistical analysis. We performed a similar analysis using relative increases over baseline (0 min) for each mutant line and Col-0. We found that JA, SA, and ABA levels in some MIPP and MAPK mutants were different than in Col-0.

Compared to Col-0, wound-induced levels of the wound hormone JA were altered in the *mpk6* and *mkp1* mutants (Fig. 4 A, D, H, I). In the *mpk6* mutant, median ng/g FW was significantly lower at 30 min (*H, mpk6*=619 ng/g FW, Col-0 =726 ng/g FW, p * =*0.031,* Wilcoxon Signed Rank Test [WSRT); this trend was replicated at 180 min (*J,* median *mpk6*=728 ng/g FW, Col-0 =1178 ng/g FW) but $n = 3$ provided only 75% actual confidence, too low to establish significance (Appendix B.2.1.2). Conversely, median JA levels in the *mkp1* mutant were higher in all three timepoints; at 30 min (*mkp1*=857 ng/g FW, Col-0 =726 ng/g FW, $n = 6$) and at 180 min (*mkp1*=1603 ng/g FW, Col-0 =1178 ng/g FW, n = 3) the effect was not found to be significant, but significance was detected at 90 min (*mkp1*=1074 ng/g FW, Col-0 =846 ng/g FW, $n = 6$, p * =*0.03*, WSRT, Appendix B.2.1.2). In Col-0 and the mutants, the highest JA levels were detected at 180 min, except for *mpk6* where they were reached at 90 min

To discern overall differences in wound-induced hormone accumulation between Col-0 and the mutant plants, we compared the combined values from each time point post wounding in the mutants as fold over Col-0 (=1) (Fig. 4 *K*). We found that the *mkp1* mutant showed a significant overall increase in the median fold accumulation of JA compared to Col-0 (*mkp1* =1.2, n = 17, p * *=*0.006*). We also observed an overall decrease in the *mpk6* mutant (*mpk6* =0.84), but the difference was not significant (p = 0.26, WSRT). Differences in initial levels (0 min) were not significantly different between all lines (Fig. 4 *G*). Since data for the 0 min time point show some variability among lines, we also calculated relative JA abundance for each time point compared to the 0 min time point (baseline) for each mutant line and Col-0 (Fig. 4 *L)*. The *pp2c5* mutant showed a reduced relative abundance (Col-0 =183, *pp2c5* =117, p * **=*0.0001,* WSRT*)*, likely due to slightly elevated JA at time 0′ compared to Col-0 (Fig. 4, *L*); relative abundance was similar to that of Col-0 for other lines, with the exception of the *mkp1* mutant which showed a slight increase without significance (*mkp1* =234, $p = 0.16$). Taken together, our analyses indicate that changes in JA accumulation in response to wounding only occurred in the *mkp1* mutant, where we observed a slight increase in JA compared to Col-0, and in the *mpk6* mutant, where we observed a slight decrease in JA compared to Col-0. (Appendix B.2.1.3).

Salicylic acid (SA) accumulates in response to stressors like pathogens and aphids, but not wounding. We tested whether SA levels in MIPP mutants would change in response to wounding, which would indicate a disruption in wound signaling. No reports addressing SA levels in response to wounding are available for the MIPP mutants. The SA pathway is known to repress JA signaling via interference of SA master regulator NPR1 (*NONEXPRESOR OF PR GENES 1*) with the JA master regulator MYC2 (Nomoto et al. 2021). However, direct involvement of MAPKs in this JA/SA crosstalk is not known.

In wounded Col-0 plants, SA concentrations do not change significantly. At 30 and 90 min after wounding, a minor dip in SA levels can be detected in Col-0 (Fig. 5, A-F). This could be due to suppressive crosstalk from JA (Wei et al. 2014), which is already accumulating strongly at 30 min after wounding (Fig. 4 A-F). The mutants *mpk6, mpk3*, *mkp1* and *ap2c1* show higher SA levels than Col-0 at time 0. This correlates with a stronger dip effect at 30 min in these lines (Fig. 5 A, B, D, F). The sample size for 0 min (n = 4 biological replicates) was too small to determine significant differences amongst all genotypes (Fig. 5 G, Appendix B.2.2.2). At 90 min, SA levels in Col-0 are similar to those at 0 min. In

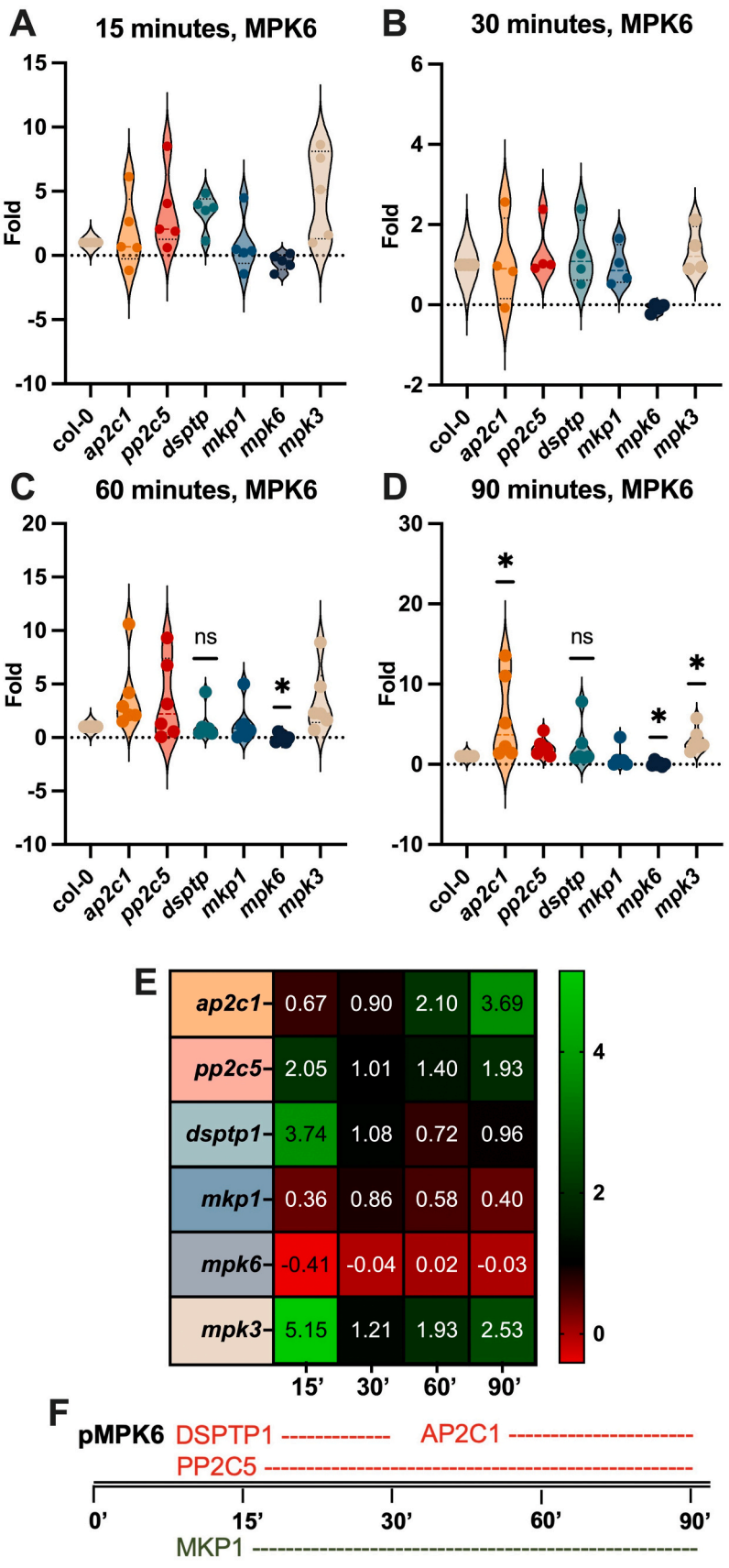

(caption on next page)

Fig. 2. Quantification of immunoblot signals shows that wound-induced MPK6 phosphorylation kinetics are negatively regulated by AP2C1, PP2C5, and DsPTP1, but not MKP1. Signals from immunoblots (Fig. 1, A.2.1 - A.2.5) were quantified, signal intensities in mutants were expressed as fold over Col-0 (Col-0 = 1), and significance was calculated using Wilcoxon Signed Rank test (WSRT) (Appendix B.1.1). Points plot single signals generated from one protein sample containing 10 plants. Black dotted lines on violins indicate quartiles of median. Fold MPK6 phosphorylation above Col-0 is shown at 15 min ($n = 5$ biological replicates) (A), 30 min ($n = 4$) (B), 60 min ($n = 6$) [*mpk6, ap2c1* $p * = 0.03$] (C), and 90 min ($n = 6$) [*Pp2c5, ap2c1, mpk6,* $p * = 0.031$, *mpk3,* $p * = 0.03$] (D). (E) Heat map reporting median value for each line at each time sampled. (F) Timing of MAPK6 dephosphorylation by MIPPs based on numbers shown in E. Red indicates negative regulation, and green indicates positive regulation by wild type MIPPs.

contrast, in the *mpk6*, *mkp1* and *ap2c1* mutants (Fig. 5, A, D, F), elevated SA levels were detected at 90 min, although JA levels were still increasing after 90 min. This indicated that in these three mutants, wound-induced JA and SA levels were at least partially uncoupled, indicating a role for MPK6, MKP1, and AP2C1 in JA-SA crosstalk. In contrast to *mpk6*, SA levels at 90 min in the *mpk3* mutant (Fig. 5 B) were similar to levels in Col-0, showing that MPK6 and MPK3 regulate SA accumulation in response to wounding differently. However, median fold SA levels in *mpk3*, when all time points post wounding were combined, are elevated compared to Col-0 (*mpk3* =1.33, $p * * = 0.009$, n = 12, WSRT, Fig. 5 J), showing an MPK3 effect on SA synthesis (Appendix B.2.2.3).

Wound-induced SA levels in *mkp1* and *mpk6* mutants were significantly elevated at 30 min and 90 min post wounding as compared to SA levels in Col-0. At 30 min, the median value for *mkp1* was 224 ng/g FW, and the median value for Col-0 was 132 ng/g FW (n = 6, $p * = 0.03$, WSRT, Fig. 5 H, Appendix B.2.2.2). At 90 min, the median value for *mkp1* was 355 ng/g FW and the median value for Col-0 143 ng/g FW (n = 6, $p * = 0.03$, WSRT; Fig. 5 I, Appendix B.2.2.2). For *mpk6*, the numbers were as follows: 30 min: 239.6 ng/g FW, Col-0 = 132 ng/g FW, Fig. 5 H); 90 min (243 ng/g FW, Col-0 =143 ng/g FW, Fig. 5 I). These differences approached significance (p = 0.09 and p = 0.06,

$n = 6$ for both time points, WSRT, Appendix B.2.2.2). In *mkp1, mpk3,* and *mpk6* mutants, median fold SA levels in *mpk3* at all time points combined were also elevated (*mkp1* =1.76, $p * * = 0.001$; *mpk3* =1.33, $p * * = 0.009$; *mpk6* =1.35, $p * = 0.027$; Col-0 =1, n = 12 all lines, WSRT, Appendix B.2.2.3, Fig. 5 J). While the *pp2c5* mutant showed no significant differences in SA levels compared to Col-0 at any time, it was the only line to show unusual accumulation over baseline (*pp2c5* =1.31, n = 14, Col-0 =0.88, n = 14, $p * = 0.02$, WSRT, Appendix B.2.2.3, Fig. 5 K), possibly due to decreased SA levels at 0 min and no suppression effect at 30 min. This indicates that PP2C5 may contribute to suppressing SA synthesis at 30 min after wounding. We detected significantly higher median SA in the *dsptp1* mutant at 30 min (160 ng/g FW), but this effect was likely caused by a large outlier visible on the plot (Fig. 5 H). Taken together, we observed noticeable and significant changes in constitutive SA levels (0 min) and in SA accumulation in response to wounding in some of the mutants. Notably, *mkp1*, *mpk6*, *mpk3*, and possibly *pp2c5* showed elevated SA levels.

Abscisic acid (ABA) levels rise in response to wounding (Heyer et al. 2018; Birkenmeier and Ryan, 1998) and changes in leaf turgor (Sussmilch et al. 2017), and support JA signaling in defense against herbivores (Vos et al. 2013). ABA levels showed an increase at 30 min post wounding, peaked at 90 min, and leveled off by 180 min (Fig. 6, A-F). More data points are required to establish statistical significance at some time points (Appendix B.2.3.2), but medians reported for some mutants suggest some biologically relevant effects are present. The *mkp1* mutant showed reduced median ABA at 30 min (*mkp1* =2.58 ng/g FW, $n = 6$; Col-0 =4.74 ng/g FW, $n = 6$; p = 0.16, Fig. 6 *H)* and 90 min (*mkp1* =8.23 ng/g FW, $n = 5$; Col-0 =9.39 ng/g FW, $n = 6$; $p = 0.13$, Fig. 6 *I*). Median fold ABA levels in *mkp1* at all time points combined compared to Col-0 were also significantly reduced in this mutant (*mkp1* =0.84, $n = 16$; Col-0=1, $n = 17$; $p * = 0.018$, WSRT, Appendix B.2.3.3, Fig. 6 K*)*. Conversely, we detected high median ABA in the *mpk3* mutant at 90 min (*mpk3* =13.1 ng/g FW, $n = 6$; *Col-0* =9.39 ng/g FW, $n = 6$; p = 0.16, Fig. 6 I*)* and 180 min (*mpk3* =12.6 ng/g FW, $n = 3$; Col-0=8.46 ng/g FW, $n = 3$; p = 0.25, Fig. 6 J). Median fold ABA levels in *mpk3* at all time points combined compared to Col-0 was slightly elevated, and the result only approached significance (*mpk3* =1.14, $n = 17$; Col-0=1, $n = 17$; p = 0.07, WSRT, Appendix B.2.3.3, Fig. 6 K). However, it should be.

for ABA levels by LC-MS. (A-F) Time courses of mean ABA concentrations (pmol/g fresh weight) in Col-0 and mutant plants post wounding. Error bars plot SEM. (G-J) Comparison of mean ABA concentrations (ng/g fresh weight) in Col-0 and mutant plants at each time point post wounding. Dashed lines in violin plots show median, and dotted lines show quartiles based on multiple biological replicates ($n_{0'}$=4, $n_{30'}$=5–6, $n_{180'}$=3). Significance was calculated using WSRT, $p * \leq 0.05$. The 180-minute time point had too few values to reach 95% AC (75%). (Appendix B.2.3.2) (K) Comparison of fold ABA levels combined from each time point in mutant plants relative to Col-0 (= 1-fold). Significance was calculated by WSRT, $p * \leq 0.05$ (Appendix B.2.3.3).

noted that elevated ABA levels in *mpk3* were detected at both relevant time points post-wounding (90 and 180 min). The *dsptp1* mutant showed remarkably high median ABA at 180 min (*dsptp1* =12.6 ng/g FW, $n = 3$; Col-0 =8.5 ng/g FW, n = 3; p = 0.25, WSRT, Appendix B.2.3.2, Fig. 6 J), although the sample size was too small to establish statistical significance. Due to non-detect instances in some replicates at 0 min for ABA, we did not consider the pre-wounding value for each line a useful baseline for analysis over all times. Taken together, we found that wound-induced ABA levels peaked at 90 min and then levelled off in Col-0, whereas this time course was slightly altered in *mpk3* (Fig. 6 B), *mkp1* (Fig. 6 D), and *dsptp1* (Fig. 6 E) mutants. An alternate figure containing all hormone results post wounding plotted as individual values are shown in Figure A.7.

3.3. Larval Growth Assays

Since we determined differences in wound-induced MAPK kinetics and defense hormone accumulation in *mpk6*, *mpk3*, and MIPP mutants, which are relevant parameters for defenses against herbivores, we tested whether these changes would correlate with altered weight gain in lepidopteran larvae. Larvae grow faster on mutants defective in JA signaling or JA synthesis than on wildtype plants (Hoo et al. 2008; Zhang et al., 2015). High SA levels may suppress JA signaling, reducing the effectiveness of the wound response (Van der Does et al. 2013; Verhage et al., 2011). Defective ABA synthesis also compromises resistance against herbivorous insects (Vos et al. 2013).

We raised neonates of the generalist *Trichoplusia ni* (cabbage looper, Lepidoptera), which prefers Brassicaceae, on our MIPP and MAPK knockout mutants in no-choice experiments, i.e., each neonate larva was confined to the same group of 2-week-old plants ($n = 8$ plants) until pupation. Larval weight was measured 12 and 14 days after hatching. Care was taken to avoid weighing larvae during the pre-pupation phase, in which larvae lose frass weight. Median larval weights at day 12 were significantly reduced in *mpk6* and *dsptp1* mutants (Col-0 mean=79 mg, median=67 mg, $n = 39$; *mpk6* mean=61 mg, median=57 mg, $n = 39$, $p*$=0.012; *dsptp1* mean=55 mg, median=57 mg, $n = 39$, $p**$=0.0081; Fig. 7 A; WSRT; Appendix B.3.1). On day 14, all cohorts but the *ap2c1* cohort showed significantly reduced weight (Col-0 mean=168 mg, median=180 mg, $n = 35$; *mpk6* mean=134 mg, median=140 mg, $n = 38$, $p****\leq 0.0001$; *dsptp1* mean=138 mg, median=148 mg, $n = 34$, $p****\leq 0.0001$; *mpk3* mean=156 mg, median=165 mg, $n = 38$, $p**$=0.0051; *pp2c5* mean=140 mg, median=138 mg, $n = 38$, $p****\leq 0.0001$; *mkp1* mean=158 mg, median=166 mg, $n = 37$, $p***$=0.0004; WSRT, Appendix B.3.2, Fig. 7 *B*). These results indicate

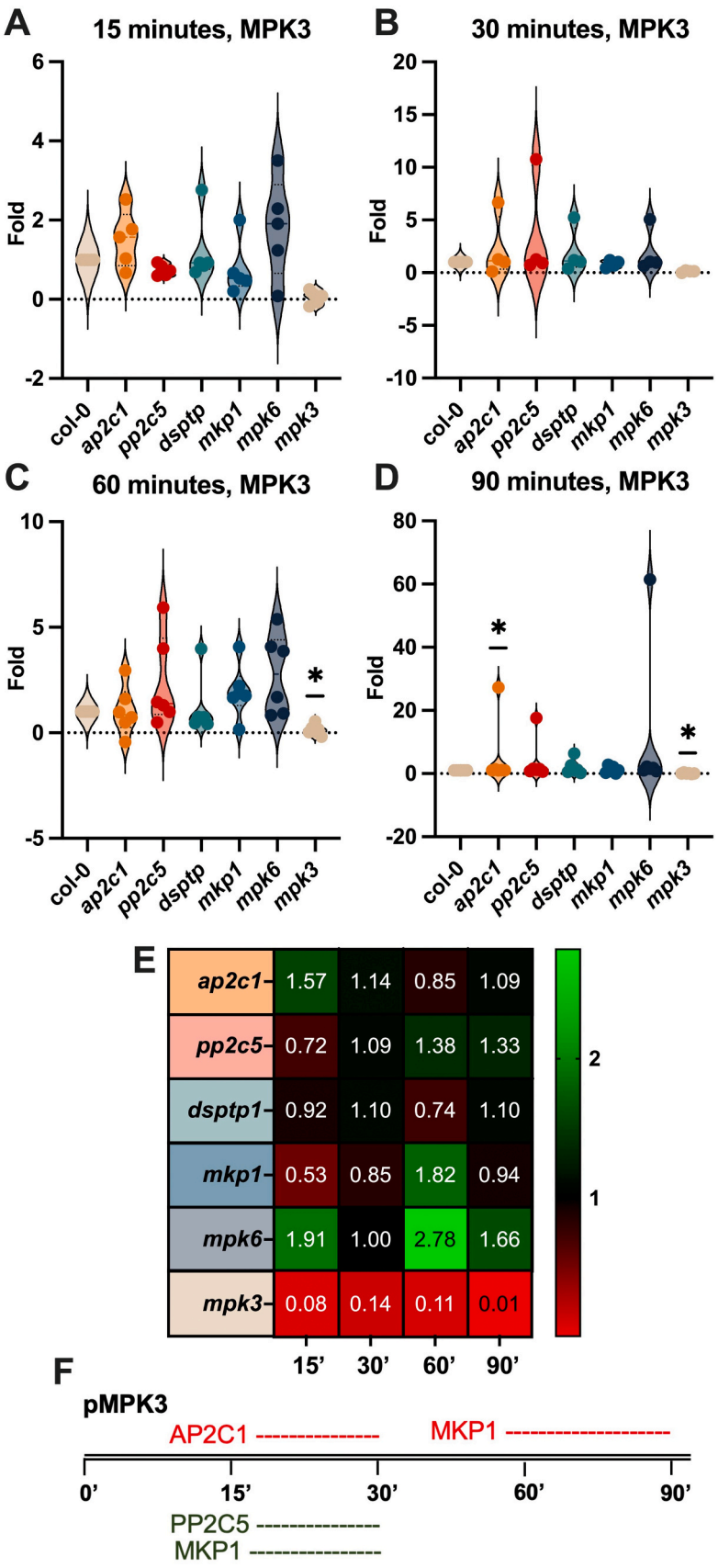

(caption on next page)

Fig. 3. Quantification of immunoblot signals shows that wound-induced MPK3 phosphorylation kinetics are negatively regulated by AP2C1 and MKP1. Signals from immunoblots (Fig. 1; A.2.1 - A.2.5) were quantified, signal intensities in mutants were expressed as fold over Col-0 (Col-0 = 1), and data were analyzed by WSRT. (Appendix B.1.2). Points plot single signals generated from one protein sample containing 10 plants. Black dotted lines on violins indicate quartiles of median. Fold MPK3 phosphorylation above Col-0 is shown at 15 min ($n = 5$ biological replicates) (A), 30 min ($n = 4$) (B), 60 min ($n = 6$) [*mpk3* $p * = 0.03$] (C), and 90 min ($n = 6$) [*ap2c1, mpk3,* $p * = 0.03$] (D). (E) Heat map reporting median value for each line at each time sampled. (F) Timing of MAPK6 dephosphorylation by MIPPs based on numbers shown in E. Red indicates negative regulation, and green indicates positive regulation by wild type MIPPs.

that MPK6/3, PP2C5, MKP1, and DsPTP1 negatively regulate resistance of Arabidopsis against *T. ni*, although MPK3/6 kinetics and defense hormone levels are affected in different ways by mutations in different MIPP genes.

We also tested the effects of MPK6/3 misregulation on larval growth of the generalist *Spodoptera exigua* (beet armyworm), which has no preference for Brassicaceae. Larvae were raised for 7 days on artificial medium and then transferred to plants (n = 260 plants/line/biological replicate) to complete growth to pupation (6 additional days). Larvae (n = 12/biological replicate/genotype, 5–7 replicates/genotype) were isolated in covered boxes (no choice) on a lawn of plants and weighed each day until pupation. Defense effects on larval weight were measurable during the last three days before pupation, on days 10 to 12 (Fig. 8 A-C). On day 10, larvae in the *pp2c5* cohort (*pp2c5* median=65 mg, mean=68 mg, SEM=2.2, $p * ** *** \leq 0.0001$) and the *ap2c1* cohort (*ap2c1* median=60 mg, mean=64 mg, SEM=2.1, $p * * = 0.004$) had increased weight compared to those in the Col-0 cohort (Col-0 median=56 mg, mean=60 mg, SEM=2.4; WSRT, Appendix B.4.1, Fig. 8 A). By day 11, those in the *mkp1*, *dsptp1*, and *mpk3* cohorts also showed increased weight over Col-0 (Col-0 median=96 mg, mean=99 mg, SEM=3.4; *mkp1* median=105 mg, mean=109 mg, SEM=4.2, $p * * = 0.005$; *dsptp1* median=102 mg, mean=102 mg, SEM=3.3, $p * = 0.049$; *mpk3* median=109 mg, mean=107 mg, SEM=4.2, $p * = 0.01$), along with the *pp2c5* and *ap2c1* cohorts (*pp2c5* median=119 mg, mean=121 mg, SEM=4.3, $p * *** \leq 0.0001$; *ap2c1* median=103 mg, mean=104 mg, SEM=3.5, $p * = 0.02$; Fig. 8 B; WSRT, Appendix B.4.2). On day 12, larvae in all cohorts except *dsptp1* and *mpk6* had significantly higher weights compared to Col-0 (Col-0 median=137 mg, mean=137 mg, SEM=3.63), including the *ap2c1* cohort (*ap2c1* median=149 mg, mean=144 mg, SEM=4.5, $p * = 0.02$), the *pp2c5* cohort (*pp2c5* median=164 mg, mean=156 mg, SEM=5.6, $p * * = 0.001$), the *mkp1* cohort (*mkp1* median=162 mg, mean=159 mg, SEM=5.55, $p * *** \leq 0.0001$) and *mpk3* cohort (*mpk3* median=161 mg, mean=159 mg, SEM=5.53, $p * * = 0.001$; WSRT, Appendix A.4.2; Fig. 8 C; WSRT, Appendix B.4.3).

S. exigua experiments proved to be challenging to evaluate due to early pupation. *S. exigua* larvae burrow in preparation for pupation and could not be weighed without disrupting the experiment. By the end of each experiment, on day 13, larvae on some mutant plants had undergone pupation, while many of the larvae raised on Col-0 were still feeding. A high early pupation rate confounded the analysis of larval weight gain on day 13. In Lepidopterans, pupation is size-dependent (Nijout et al., 2014), with faster growing larvae pupating earlier than slower growing larvae, although other factors triggering pupation cannot be excluded. To link larval weight and pupation, we counted the number of larvae that had pupated on each day. On days 11 and 12, the *dsptp1* mutant showed a pupation delay; conversely *mpk3* and *mpk6* mutants showed accelerated pupation starting at day 11, which became highly significant on day 12 (Fig. 9, A-C; WSRT, Appendix B.4.4.1). The pupation rate for each day is reported in Fig. 9 D. In a 2-way ANOVA analysis including pupation on all days, the *mpk3* cohort showed an increased mean pupation rate compared to Col-0 (*mpk3*= −0.268, $n = 24$; Col-0 = −0.16, $n = 34$; $p * = 0.017$, Dunnett's multiple comparisons test). A stronger effect was observed in the *mpk6* cohort (n = 24, mean= −0.297, $p * * = 0.0018$, Dunnett's multiple comparisons test). The cohort raised on *pp2c5* plants showed an elevated pupation rate compared to Col-0 on Day 12 and 13, but the effect was not present throughout the time course (*pp2c5* = −0.217, n = 29; p = 0.297, Dunnett's multiple comparisons test). No significant interaction was demonstrated between day and genotype effects in the 2-way-ANOVA (day/genotype, p = 0.26). This indicates that significant differences in pupation rate between larvae feeding on Col-0 and *mpk6* ($p * * = 0.002$) or Col-0 and *mpk3* ($p * = 0.02$) were detectable throughout the feeding time course and not affected by measurement day. The shorter time to pupation may indicate less effective plant defenses against larvae feeding on *mpk6* and *mpk3* mutants than on Col-0 plants. Taken together, these results support that misregulation of MPK6/3 activity affects the time from hatching to pupation of *S. exigua* larvae.

4. Discussion

Through dephosphorylation of MAPKs, MIPPs can regulate the activation time, amplitude, and duration of MAPK signaling, resulting in input-specific patterns of MAPK kinetics. We tested the effect of four different MIPPs on MAPK kinetics and found that their effects are different, most likely due to MIPP-specific timing of phosphatase activity in relation to MAPK activity (Fig. 10). As expected, MPK6 or MPK3 activity was stronger and/or more prolonged in the MIPP knockout mutants *pp2c5*, *dsptp1*, and *ap2c1* than in Col-0 plants. Surprisingly, in *mkp1* mutant plants, MPK6 activity was lower for MPK6 over the entire 90 min time course and for MPK3 at 15 and 30 min. Other reports showed stronger wound-or molecular pattern-induced MPK6/3 activity in *mkp1* mutants but also did not find prolonged MAPK activity, as can be expected for a MIPP mutant. Rather, these reports found a more transient MAPK activity (Escudero et al. 2019; Ayatollahi et al. 2022; Anderson et al. 2011). The cause for the low MAPK activity in *mkp1* mutant plants is unknown but may point to an overcompensation by another wound-responsive MIPP. MPK3 activity was elevated over Col-0 in *mkp1* at 60 min after wounding, which is consistent with a function of MKP1 as a MIPP. We also included the *mpk3* and *mpk6* null mutants and found that the activity of the intact MPK was upregulated in plants mutated for the other MPK. Since both MAPKs share many substrates and are known to function together in stress responses, overcompensation of one MPK in the mutant of the other MPK may effectively negate the effect of the null mutation, at least in pathways where MPK3 and MPK6 have redundant functions (Ichimura et al. 2000; Rayapuram et al. 2018). We will consider this for the interpretation of hormone and herbivory data.

In tomato and tobacco, orthologs of Arabidopsis MPK6/3 positively regulate JA synthesis in response to wound and herbivory-related signals (Kandoth et al. 2007; Wu et al. 2007). In contrast, MPK6/3 activity in Arabidopsis can be induced by JA treatment, indicating a species-specific function of MPK6/3 in JA synthesis and signaling (Takahashi et al. 2007). ABA signaling has been shown to amplify JA signaling in response to wounding (Vos et al. 2013), whereas SA signaling can repress JA signaling (Nomoto et al. 2021). The JA and SA pathways share few stress gene targets and generally repress one another at both the hormone synthesis and target gene levels (Van der Does et al. 2013; Wei et al. 2014). Except for the *mkp1* mutant, which showed elevated wound-induced JA accumulation, we did not find significant effects on JA synthesis in the MAPK and MIPP mutants, although *mpk6* showed slightly lower JA levels than Col-0 (Fig. 10). This indicates that MAPKs are not directly involved in JA synthesis in Arabidopsis. The increased JA accumulation observed in the *mkp1* mutant, along with its low MPK6 activity post wounding, is consistent with previous reports implicating MPK6 as a negative regulator of JA signaling (Takahashi et al. 2007).

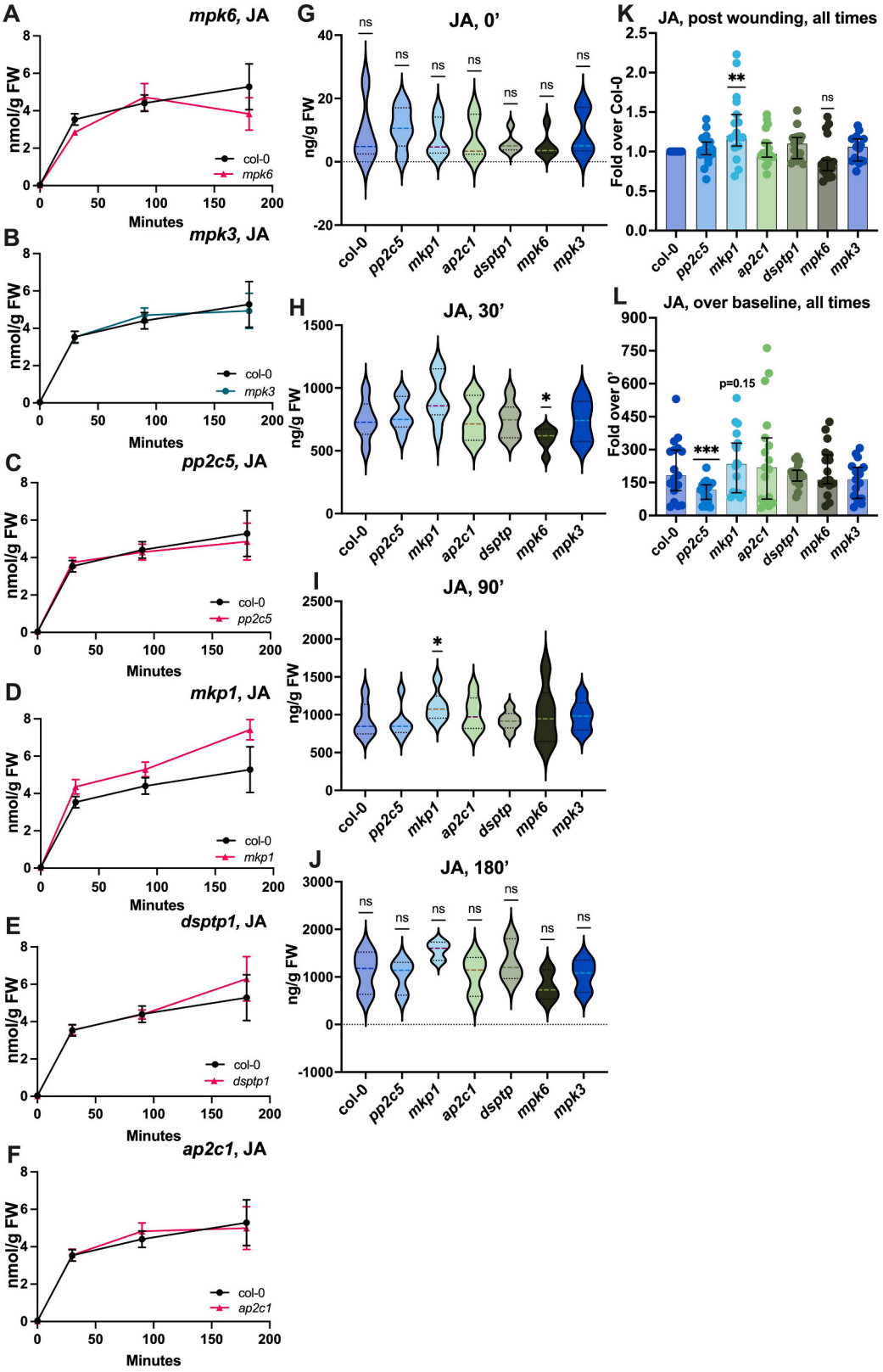

Fig. 4. Wound-induced JA accumulation is changed in *mpk6* and *mkp1* mutants. 3-week-old Col-0 and mutant plants were wounded with forceps and analyzed for JA levels by LC-MS at the times indicated. (A-F) Mean hormone concentrations (nmol/g fresh weight) over a 180 min time course. Error bars plot standard error of the mean (SEM). (G-J), Violin plots show comparison of mean JA concentrations (ng/g fresh weight) in Col-0 and mutant plants at each time point post wounding. Dashed lines plot median, dotted lines plot quartiles. Biological replicates ($n_{0'}$=5, $n_{30'}$=6, $n_{90'}$=6, $n_{180'}$=3) were collected on separate days from separate plant cohorts. Significance was calculated using WSRT, p * $\leq$0.05. 180-minute time point had too few values to reach 95% confidence (75%, Appendix B.2.1.2). (K) values relative to Col-0, at all times post wounding; WSRT. (L) Fold values relative to baseline (0') measurement. WSRT, p * *$\leq$0.01, p * ** $\leq$0.001. Dots plotted over bars in (K) and (L) represent individual replicates included in the analysis. Data in (K) and (L) include results shown in A-J, plus two 60 min data sets (Appendix B.2.1.3).

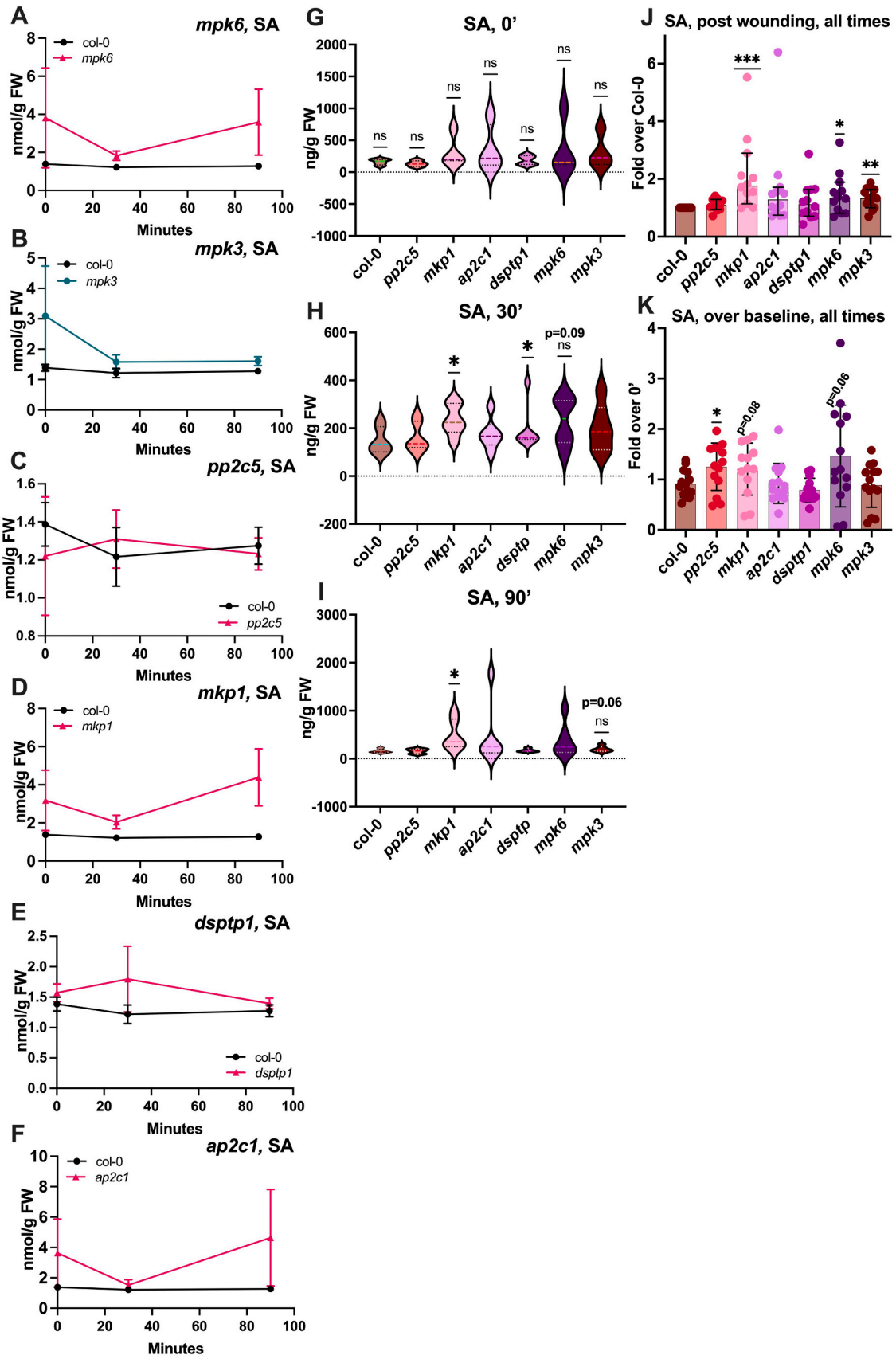

(caption on next page)

Fig. 5. Wound-induced and constitutive SA accumulation is changed in *mkp6, mpk3* and *mpk1* mutants. 3-week-old Col-0 and mutant plants were wounded with forceps and analyzed for SA levels by LC-MS. (A-F) Time courses of mean SA concentrations (nmol/g fresh weight) in Col-0 and mutant plants post wounding. Error bars plot SEM. Error bars for SA in Col-0 in *A, B, D & F* are invisible due to scale. (G-I) Comparison of mean SA concentrations (ng/g fresh weight) in Col-0 and mutant plants at each time point post wounding. Dashed lines in violin plots show median, and dotted lines show quartiles based on multiple biological replicates ($n_{0'}$=4, $n_{30'}$=6, $n_{90'}$=6). Significance was calculated using WSRT, p * ≤0.05. (Appendix B.2.2.2) (J) Comparison of fold SA levels combined from each time point in mutant plants relative to Col-0 (= 1-fold). (K) Relative SA abundance for each time point compared to time = 0 (baseline) for each mutant line and Col-0. Significance was calculated by WSRT, p * ≤0.05, p * *≤0.01, p * ** ≤0.001. Dots plotted over bars in (J) and (K) represent individual replicates included in the analysis. Results in (J) and (K) include results shown in A-I, plus two 60′ results. (Appendix B.2.2.3).

On the other hand, the two MIPP mutants *mkp1* and *pp2c5,* and the MAPK mutants *mpk6* and *mpk3*, had higher wound-induced SA accumulation than Col-0. The *dsptp1* and *ap2c1* mutants had neither elevated JA nor SA levels, indicating that these two MIPPs play no role in wound-induced JA and SA synthesis (Fig. 10). ABA levels were significantly reduced in *mkp1*, and only slightly elevated in *mpk3* and *dsptp1*. Therefore, levels of the two positively interacting hormones JA and ABA were not significantly altered in all mutants but *mkp1*. In *mkp1*, both JA and SA are higher, while ABA levels are lower than in Col-0, indicating that MKP1 has a different effect on MAPK kinetics and hormone synthesis than all other MIPPs (Fig. 10).

Not much is known about the role of MPK6/3 in responses to chewing herbivorous insects in Arabidopsis. Since caterpillars mechanically wound leaves with their mandibles, this should lead to activation of MAPKs, as demonstrated for tomato and *N. attenuata* (Kandoth et al. 2007; Wu et al. 2007). To our knowledge, there is only one relevant study where the authors show that *S. littoralis* caterpillars clearly activate MPK2 but not or only weakly MPK6 and MPK3 (Sözen et al. 2020). MPK2 also responds to ABA (Danquah et al. 2015). MIPPs that may downregulate MPK2 activity are not known. MPK2 is a member of MAPK subgroup C, while MPK6/3 belong to subgroup A. Nevertheless, it cannot be excluded that the four MIPPs studied here also dephosphorylate MPK2. We therefore explored whether misregulation of MPK6/3 activity by our four MIPPs would correlate with changes in Arabidopsis responses to larvae of two lepidopteran species.

The strongest difference we observed was that *T. ni* larvae gained less weight on all mutant plants but *ap2c1*, while *S. exigua* larvae showed increased weight on all mutants except *dsptp1* and *mpk6* (Fig. 10). This indicates that the two species respond differently to Arabidopsis defenses, though both are members of the Noctuidae family and have a similar lifestyle (Capinera, 2020). However, it cannot be excluded that the differences are due to experimental design. A more extended exposure to *T. ni* (days 2 to 14 post-hatching vs. days 6 to 12 for *S. exigua*) that started feeding as very small larvae may have induced a more intense defense response in *Arabidopsis*. Along the same line, *S. exigua* larvae that started feeding at a larger size (day 6) encountered naïve plants that were overwhelmed by an attack of already grown larvae and had less time to deploy defenses. Nevertheless, resistance to these caterpillars was altered by mutations in MAPK and MIPP genes. Loss-of-function of *MPK3*, *MKP1*, and *PP2C5* resulted in higher resistance to *T. ni* (lower weight) and lower resistance to *S. exigua* (higher weight) as compared to Col-0. In contrast, loss-of-function of *DsPTP1* did not affect resistance to *S. exigua*, but increased resistance to *T. ni.* Loss-of-function of *AP2C1* also caused opposite effects on resistance; resistance to *S. exigua* was reduced, but unaffected in response to *T. ni*. We also measured the pupation rate of *S. exigua*, since larvae on *mpk3* and *mpk6* mutants pupated faster than larvae on Col-0 reducing the number of larvae that could be measured for the growth experiment (Fig. 8). Increased weight and shortened larval stage corresponded only when larvae were feeding on *mkp3* and *pp2c5* mutant plants (more weight gain, shorter larval period). In the *mkp1* cohort, the two parameters were disconnected. Larvae feeding on *mpk6* plants completed their larval period faster than larvae feeding on all other mutant plants. It is likely that the largest larvae in this cohort pupated sooner, making larval weights in the *mpk6* cohort not directly comparable to those raised on other mutant plants (Fig. 9 D). This increased pupation rate also indicates reduced resistance of the *mpk6* mutant to *S. exigua*.

S. exigua larvae have a lower feeding index (pupal weight divided by total weight of leaf tissue consumed) on cabbage (Brassicaceae) than on other non-Brassicaceae plants, indicating a pronounced susceptibility to defenses of cabbages (Greenberg et al. 2001). Glucosinolates are the main line of defense against chewing herbivores in Brassicaceae, including *Arabidopsis thaliana*, and their synthesis is regulated by JA (Yan and Chen, 2007). Assuming a suppression of glucosinolate synthesis by SA counteracting JA signaling, mutants with higher SA levels should have lower glucosinolates and thus lower resistance to *S. exigua*. This is what we observed for *mpk3*, *mkp1*, and *pp2c5*. In contrast, *T. ni* is likely to be less sensitive to glucosinolates but may respond to other defenses in the mutants which are not suppressed by SA (regulated by JA) and reduce performance of *T. ni*. Also, while caterpillars mechanically wound leaves with their mandibles, temporal and spatial specifics of caterpillar chewing may have different effects than one-time forceps wounding as performed in our experiments (Mithöfer et al. 2005*)*.

Furthermore, herbivory results in the release of additional signals such as herbivore-associated molecular patterns and effectors, which either induce or suppress plant defenses, respectively, and thus may change MAPK kinetics and defense hormone levels (Grissett et al. 2020; Chen et al. 2019*)*. However, fatty acid-amino acid conjugates are prominent herbivore-associated molecular patterns that do not activate MAPKs and do not lead to synthesis of JA, SA, or ethylene in Arabidopsis, unlike in many other dicot and monocot families (Grissett et al. 2020; Schmelz et al. 2009). *S. exigua* contains orthologs of two effector proteins from *Helicoverpa armigera* (cotton bollworm), HARP1 and HAS1 (Prajapati et al., 2020; Chen et al. 2019; Chen et al. 2023). Therefore, it is conceivable that *S. exigua* effectors suppressed JA-mediated defenses independently of MAPK kinetics. We only measured wound-induced JA levels, so we do not know whether JA levels in herbivore-exposed plants were suppressed. Also, effectors have not been investigated for the *A. thaliana-S. exigua* system. As effectors and corresponding host plant resistance genes are often genotype-specific in both pathogens and their host plants, it is possible that the HARP1 and HAS1 proteins from *S. exigua* do not suppress Arabidopsis defenses.

Lastly, we determined whether changes in wound-induced MAPK kinetics and levels of JA, SA, and ABA could be correlated with the performance of *T. ni* and *S. exigua* larvae (Fig. 10). Mutants with high wound-induced MPK3 and low MPK6 activity include *mpk6* and *mkp1*; the two lines shared timing of peak MPK3 activity and elevated SA levels and both were similar regarding reduced resistance to both herbivore species (*mpk6* due to faster pupation, *mkp1* due to higher larval weight).

Mutants with high wound-induced MPK6 and low MPK3 activity include *mpk3*, *pp2c5*, *dsptp1,* and *ap2c1*, but times of peak MPK6 activity and duration of elevated activity are different among these mutants, e.g., *mpk3* showing an early peak and prolonged elevated MPK6 activity, while *ap2c1* showed delayed peak activity. These four mutants were different with regard to hormone synthesis and resistance to *T. ni* and *S. exigua* (Fig. 10).

The *mkp1* mutant showed wound-induced MPK6 and MPK3 activity mostly below activities in Col-0 plants, except for an increase in MPK3 activity at 60 min after wounding. These MAPK kinetics are different from all other mutant lines and unexpected for a MIPP mutant known to interact with MPK6/3, unless increased MAPK activity occurred between 0 and 15 min or after 90 min post wounding. This mutant also showed wound-induced hormone levels that were different from all other mutant lines, while at the same time showing a similar resistance

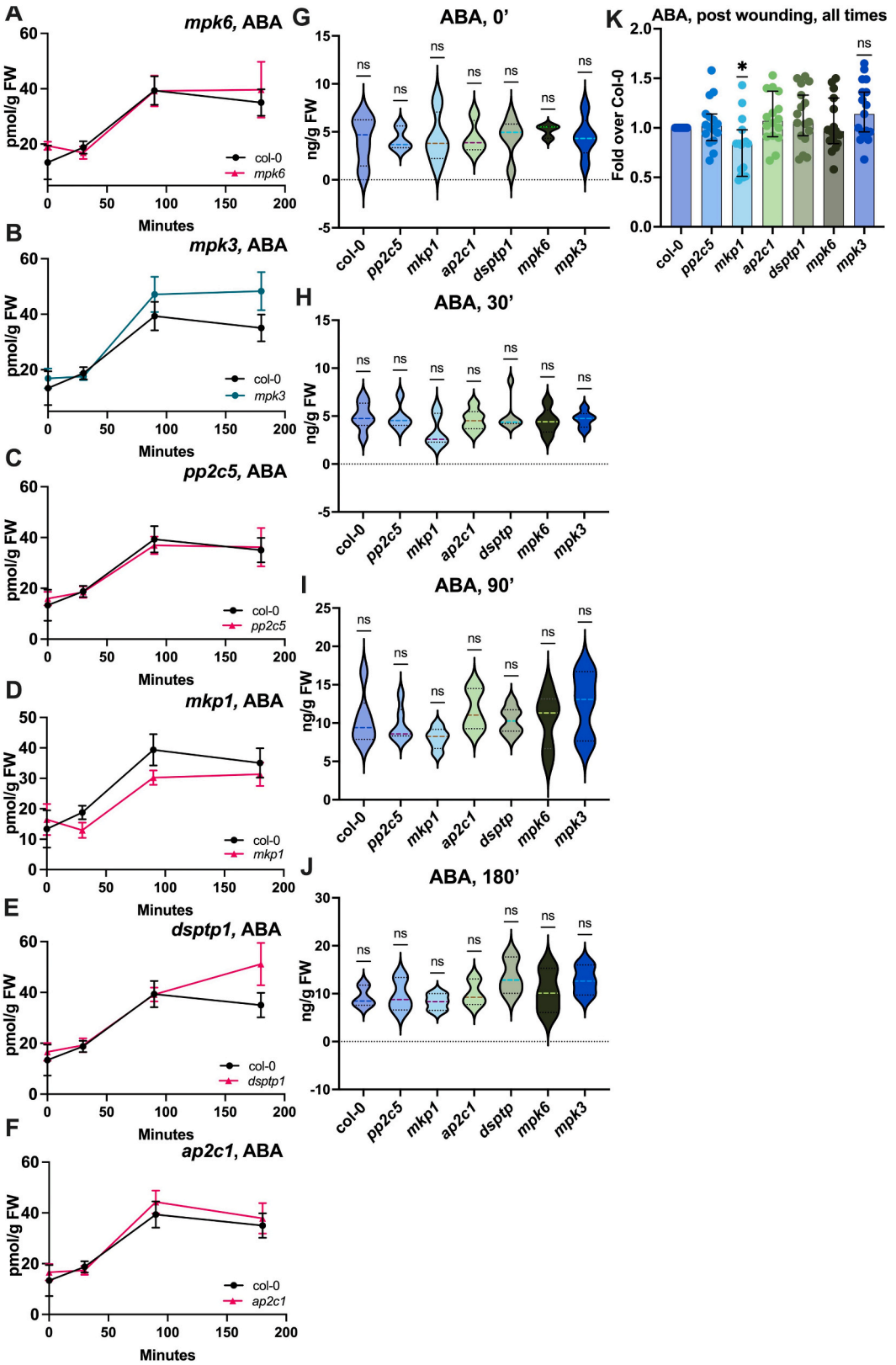

Fig. 6. Wound-induced ABA accumulation is changed in *mpk3*, *mpk1*, and *dsptp1* mutants. 3-week-old Col-0 and mutant plants were wounded with forceps and analyzed for ABA levels by LC-MS. (A-F) Time courses of mean ABA concentrations (pmol/g fresh weight) in Col-0 and mutant plants post wounding. Error bars plot SEM. (G-J) Comparison of mean ABA concentrations (ng/g fresh weight) in Col-0 and mutant plants at each time point post wounding. Dashed lines in violin plots show median, and dotted lines show quartiles based on multiple biological replicates (n 0' = 4, n 30' = 5-6, n 180' = 3). Significance was calculated using WSRT, p * $\leq$0.05. The 180-minute time point had too few values to reach 95% AC (75%). (Appendix B.2.3.2) (K) Comparison of fold ABA levels combined from each time point in mutant plants relative to Col-0 (= 1-fold). Significance was calculated by WSRT, p * $\leq$0.05 (Appendix B.2.3.3).

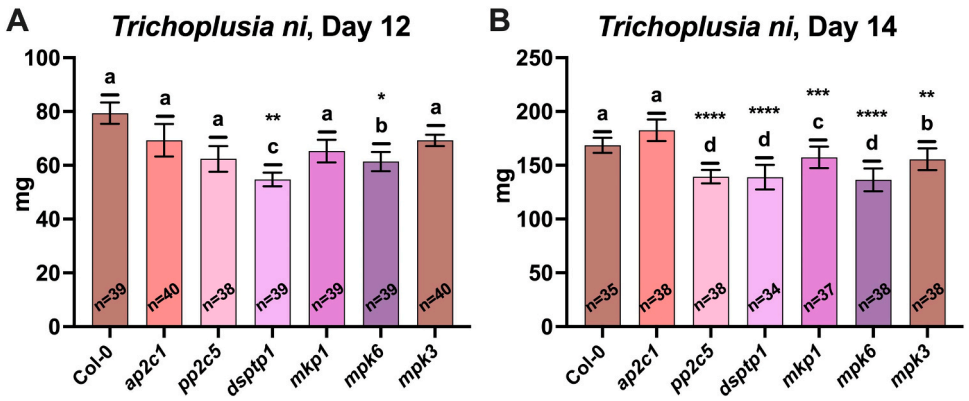

Fig. 7. Weight gain of *T. ni* larvae feeding on *mpk6*, *mpk3*, *pp2c5*, *mkp1*, and *dsptp1* mutant plants is reduced compared to Col-0. 1–2-day old *T. ni* larvae were transferred to 2-week-old Arabidopsis plants in tented boxes and allowed to feed until pupation. Larval weight was measured before pupation on day 12 and 14 after hatching (6 independent experiments with 4–5 larvae per Arabidopsis genotype each). Total *n* values used for analysis for each genotype are reported on each column. Significance calculated via WSRT; error bars show SEM. (A) Mean larval weights on day 12 ($n = 38$–40 larvae/plant genotype). Letters over bars: "b" - $p^* \leq 0.05$, "c" - $p^{**} \leq 0.01$. (B) Mean larval weights, on day 14 ($n = 24$–28 larvae/genotype; lower numbers compared to day 12 due to pupation). Letters over bars: "b" - $p^{**} \leq 0.01$, "c" - $p^{***} \leq 0.001$, and "d" - $p^{****} \leq 0.0001$. *(*Appendix B.3).

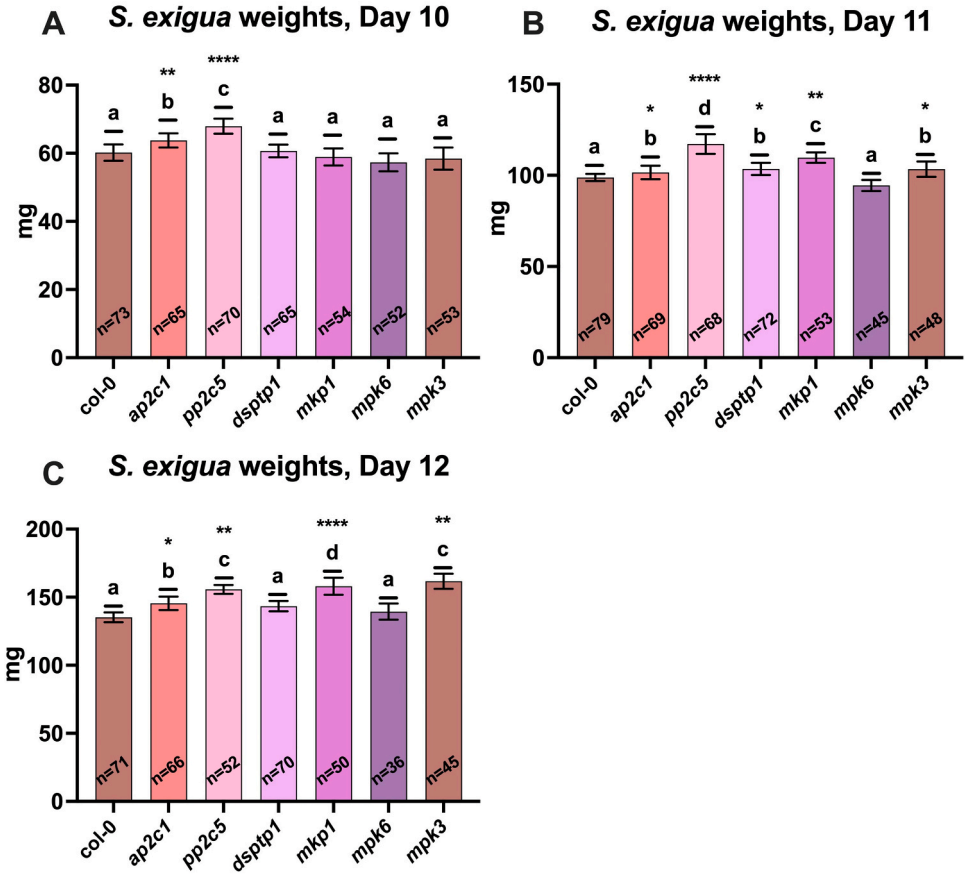

Fig. 8. Weight gain of *S. exigua* larvae feeding on *mpk3*, *ap2c1*, *pp2c5*, and *mkp1* mutant plants is increased compared to Col-0. Cohorts of 7-day old *S. exigua* larvae (n = 12) were transferred to 2-week-old Arabidopsis plants and allowed to feed until pupation (no choice). Larval weight was measured before pupation on days 10–12 after hatching (5–7 independent replicates/genotype with 12 larvae per Arabidopsis genotype each). Significance calculated via WSRT; error bars show SEM. Total *n* values entered in the analysis for each genotype are reported on each column. (A) Mean larval weights on day 10 (n = 73–52 larvae/plant genotype). Letters over bars: "b" – $p^* \leq 0.01$, "c" – $p^{***} \leq 0.0001$. (B) Mean larval weights on day 11 (n = 79–45 larvae/plant genotype). Letters over bars: "b" – $p^* \leq 0.05$, "c" – $p^{**} \leq 0.01$, "d" – $p^{***} \leq 0.0001$. (C) Mean larval weights on day 12 (n = 71–36 larvae/plant genotype). N values are lower than on day 10 and 11 due to pupation. Letters over bars: "b" – $p^* \leq 0.05$, "c" – $p^{**} \leq 0.01$, "d" – $p^{***} \leq 0.0001$. (Appendix B.4).

to *T. ni* and *S. exigua* as *mpk3* and *pp2c5* mutant plants (Fig. 10).

It is also important to note here, that knockout of either *MPK6* or *MPK3* resulted in hyperactivity of the remaining MAPK in the MPK mutants (Fig. 10). Since the functions of these two MAPKs largely overlap, we were unable to demonstrate how defenses would be altered in the absence of both MPK3 and MPK6 activity. Double mutants for

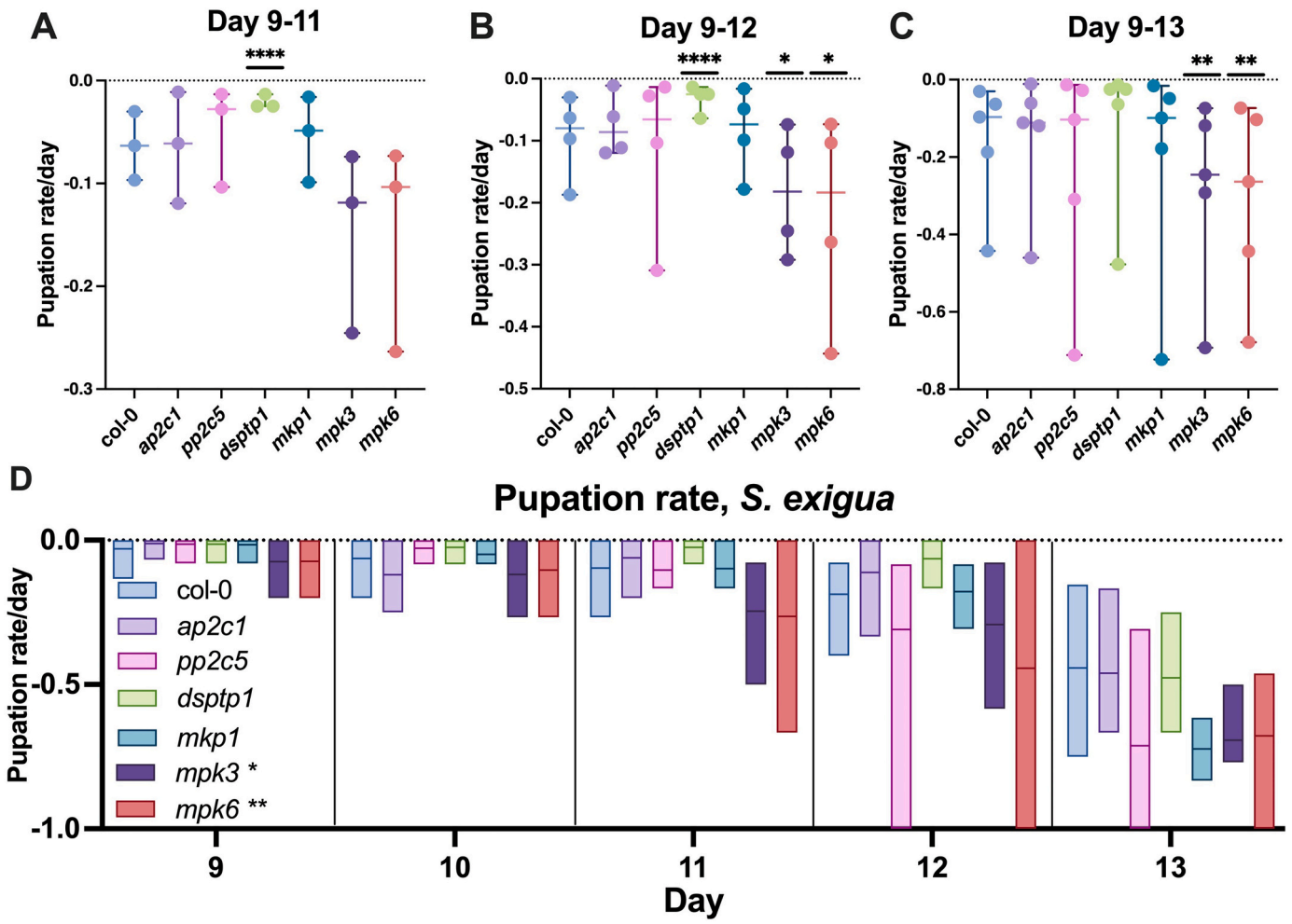

Fig. 9. Time to pupation of *S. exigua* larvae is shorter in *mpk3*, *mpk6*, and *pp2c5* mutants and longer in *dsptp1* mutants than in Col-0 plants. Larvae were raised as described in Fig. 8. (A-C) Dot plots listing one dot per day, each representing mean proportion of larvae that had pupated by the indicated day (day 9 = dot 1, day 10 =dot 2, etc.). Plots report proportion of larvae that had pupated each day during all experiments (n = 5–7 independent experiments), where − 1 represents 100% pupation and 0 reports no change. Horizontal bars show median. (A) Pupation by day 11. Col-0 vs. all lines; *dsptp1* (median = 0), p * ** *≤0.0001. (B) Pupation by day 12. Col-0 median vs. all lines; *dsptp1* (median = 0), p * ** *≤0.0001; *mpk3* (median = −0.125), p * =0.013; *mpk6* (median = −0.125), p * =0.035. (C) Pupation by day 13. Col-0 (median = −0.083) vs. all lines; *mpk3* (median=−0.168), p * *= 0.003; *mpk6* (median=−0.167), p * *= 0.0026. Significance was calculated using WSRT. (D) Box plot (low-high) of replicate values on all five days. An analysis of all values was performed (up to day 13) via 2-way ANOVA. Mutant cohort effects were analyzed by combining values for all days. Day effect on mutant cohort weight: p * ** *≤0.0001; Line effect on mutant cohort weight: p * ** *≤0.0001; Day/Line effect on mutant cohort weight: p = 0.26. Post-hoc analysis with Dunnett's multiple comparisons test reports significance on all days for *mpk3* (p * =0.017) and *mpk6* (p * *=0.0018) compared to Col-0. QQ plot associated with cohorts analyzed in 2-way ANOVA, normality, and statistical tables associated with ANOVA and WSRT are reported in Appendix B.4.4.

MPK6 and MPK3 are embryo lethal, although inducible double mutants have been generated (Zhang and Zhang, 2022). Those are hardly suitable for herbivory experiments due to unknown effects of chemical inducers of gene expression on herbivores.

In summary, we were unable to detect any obvious correlation between MPK6/3 kinetics, defense hormone levels, and resistance to two lepidopteran larvae (Fig. 10). This should not be interpreted as an absence of such a correlation. Most likely, MAPK kinetics would be altered in a more pronounced way in MIPP double and higher-level mutants, leading to stronger effects on hormone levels and resistance to herbivores.

5. Conclusions

We found that a) wound-induced MAPK phosphorylation kinetics are changed in different ways in four different MIPP mutants as compared to Col-0, resulting in MIPP-specific kinetic patterns. This may be due to a different timing of MIPP activity in relation to MAPK activity. Wound-induced levels of the defense-related hormones JA, SA, and ABA were also different in MPK6/3 and MIPP mutants, indicating that changes in MAPK phosphorylation kinetics have consequences for hormone synthesis and/or accumulation. b) We provide additional evidence that MPK6/3 are not directly involved in JA synthesis in Arabidopsis, unlike in other plant species, and we provide further evidence for a compensatory regulation of MPK6 and MPK3 activity in *mpk6* and *mpk3* mutants. c) We also found that MAPK and MIPP mutant plants showed altered resistance to *T. ni* and *S. exigua* compared to Col-0. This indicates different adaptations to Arabidopsis defenses by the two herbivore species, and that MAPKs and MIPPs are involved in regulating herbivore resistance. d) We did not find an obvious correlation between MAPK kinetics and hormone levels, and neither between hormone levels nor MAPK kinetics and resistance to the herbivores. However, in *mkp1, pp2c5, mpk6* and *mpk3* mutants, regulation of SA levels was dysfunctional leading to higher wound-induced SA levels than in Col-0. This strongly correlated with reduced resistance to *S. exigua*.

The larval growth differences we detected were statistically

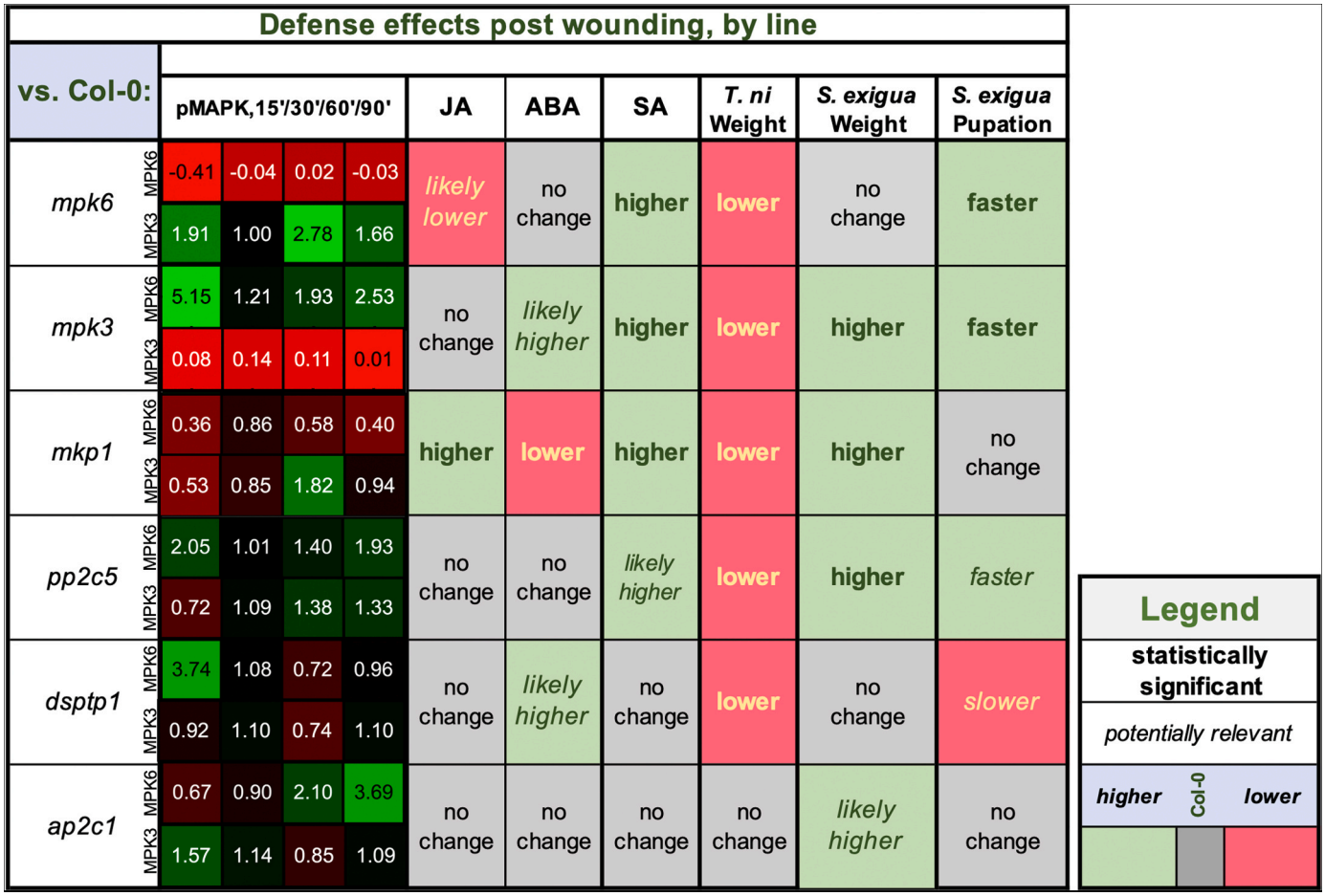

Fig. 10. Summary of defense effects associated with MAPK misregulation. Results from mutants were compared to Col-0. Further explanations are in the text.

significant, but overall relatively small. Stronger effects may emerge in higher-level MIPP mutants.

CRediT authorship contribution statement

Claire Hann: Methodology; Investigation; Formal analysis; Funding acquisition; Visualization; Roles/Writing - original draft; Writing - review & editing. Carlton J. Bequette: Investigation; Writing - review & editing.Sophia F. Ramage: Investigation. Harshita Negi: Investigation. Paula A. Vasquez: Funding acquisition, writing – review & editing, supervision. Johannes W. Stratmann: Conceptualization; Formal analysis; Funding acquisition; Project administration, Resources; Supervision; Validation; Writing - review & editing.

Declaration of Competing Interest

The authors declare that they have no known competing financial interests or personal relationships that could have appeared to influence the work reported in this paper.

Data availability

No data was used for the research described in the article.

Acknowledgements

This work was supported by the Office of the Vice President for Research, University of South Carolina (SPARC grant to C.H.; ASPIRE-I grant to P.A.V. and J.S; ASPIRE-I grant to J.W.S.). We would like to thank Drs. Michael Walla and William Cotham for invaluable help with MS analyses.

Appendix A. Supporting information

Supplementary data associated with this article can be found in the online version at doi:10.1016/j.plantsci.2023.111962.

References

J.C. Anderson, S. Bartels, M.A. González Besteiro, B. Shahollari, R. Ulm, S.C. Peck, Arabidopsis MAP kinase phosphatase 1 (AtMKP1) negatively regulates MPK6-mediated PAMP responses and resistance against bacteria, Plant J. 67 (2011) 258–268, https://doi.org/10.1111/j.1365-313X.2011.04588.x.

Z. Ayatollahi, V. Kazanaviciute, V. Shubchynskyy, K. Kvederaviciute, M. Schwanninger, W. Rozhon, M. Stumpe, F. Mauch, S. Bartels, R. Ulm, S. Balazadeh, B. Mueller-Roeber, I. Meskiene, A. Schweighofer, Dual control of MAPK activities by AP2C1 and MKP1 MAPK phosphatases regulates defence responses in Arabidopsis, J. Exp. Bot. 73 (2022) 2369–2384, https://doi.org/10.1093/jxb/erac018.

S. Bartels, J.C. Anderson, M.A. González Besteiro, A. Carreri, H. Hirt, A. Buchala, J. P. Métraux, S.C. Peck, R. Ulm, Map kinase phosphatase1 and protein tyrosine phosphatase1 are repressors of salicylic acid synthesis and SNC1 -mediated responses in Arabidopsis, Plant Cell 21 (2009) 2884–2897, https://doi.org/10.1105/tpc.109.067678.

S. Bartels, M.A.G. Besteiro, D. Lang, R. Ulm, Emerging functions for plant MAP kinase phosphatases, Trends Plant Sci. 15 (2010) 322–329, https://doi.org/10.1016/j.tplants.2010.04.003.

G.F. Birkenmeier, C.A. Ryan, Wound signaling in tomato plants: Evidence that ABA is not a primary signal for defense gene activation, Plant Physiol. 117 (1998) 687–693, https://doi.org/10.1104/pp.117.2.687.

J.L. Capinera, Handbook of vegetable pests. Handbook of Vegetable Pests, Elsevier, 2020, pp. 353–510. ⟨https://doi.org/10.1016/B978-0-12-814488-6.09988-X⟩.

C.Y. Chen, Y.Q. Liu, W.M. Song, D.Y. Chen, F.Y. Chen, X.Y. Chen, Z.W. Chen, S.X. Ge, C. Z. Wang, S. Zhan, X.Y. Chen, Y.B. Mao, An effector from cotton bollworm oral

secretion impairs host plant defense signaling, Proc. Natl. Acad. Sci. U. S. A. 116 (2019) 14331–14338, https://doi.org/10.1073/pnas.1905471116.
X. Chen, Y.Q. Liu, M.N. Wu, L. Yan, C.Y. Chen, Y.P. Mu, Y.J. Liu, M.Y. Wang, X.Y. Chen, Y.B. Mao, A highly accumulated secretory protein from cotton bollworm interacts with basic helix–loop–helix transcription factors to dampen plant defense, N. Phytol. 237 (2023) 265–278, https://doi.org/10.1111/nph.18507.
A. Danquah, A. De Zélicourt, M. Boudsocq, J. Neubauer, N. Frei Dit Frey, N. Leonhardt, S. Pateyron, F. Gwinner, J.P. Tamby, D. Ortiz-Masia, M.J. Marcote, H. Hirt, J. Colcombet, Identification and characterization of an ABA-activated MAP kinase cascade in Arabidopsis thaliana, Plant J. 82 (2015) 232–244, https://doi.org/10.1111/tpj.12808.
V. Escudero, M.Á. Torres, M. Delgado, S. Sopeña-Torres, S. Swami, J. Morales, A. Muñoz-Barrios, H. Mélida, A.M. Jones, L. Jordá, A. Molina, Mitogen-activated protein kinase phosphatase 1 (MKP1) negatively regulates the production of reactive oxygen species during Arabidopsis immune responses, Mol. Plant-Microbe Interact. 32 (2019) 464–478, https://doi.org/10.1094/MPMI-08-18-0217-FI.
G. Glauser, E. Grata, L. Dubugnon, S. Rudaz, E.E. Farmer, J.L. Wolfender, Spatial and temporal dynamics of jasmonate synthesis and accumulation in Arabidopsis in response to wounding, J. Biol. Chem. 283 (2008) 16400–16407, https://doi.org/10.1074/jbc.M801760200.
M. a González Besteiro, R. Ulm, Phosphorylation and stabilization of Arabidopsis MAP kinase phosphatase 1 in response to UV-B stress, J. Biol. Chem. 288 (2013) 480–486, https://doi.org/10.1074/jbc.M112.434654.
S.M. Greenberg, T.W. Sappington, B.C. Legaspi, T.X. Liu, M. Sétamou, Feeding and life history of *Spodoptera exigua* (lepidoptera: noctuidae) on different host plants, Ann. Entomol. Soc. Am. 94 (2001) 566–575, https://doi.org/10.1603/0013-8746(2001)094[0566:FALHOS]2.0.CO;2.
L. Grissett, A. Ali, A. Coble, K. Logan, B. Washington, A. Mateson, K. McGee, Y. Nkrumah, L. Jacobus, E. Abraham, C. Hann, C.J. Bequette, S.R. Hind, E.A. Schmelz, J. W. Stratmann, Survey of sensitivity to fatty acid-amino acid conjugates in the Solanaceae, J. Chem. Ecol. 46 (2020) 330–343, https://doi.org/10.1007/s10886-020-01152-y.
Q. Guo, Y. Yoshida, I.T. Major, K. Wang, K. Sugimoto, G. Kapali, N.E. Havko, C. Benning, G.A. Howe, JAZ repressors of metabolic defense promote growth and reproductive fitness in Arabidopsis, Proc. Natl. Acad. Sci. U. S. A. 115 (2018) E10768–E10777, https://doi.org/10.1073/pnas.1811828115.
M. Heyer, M. Reichelt, A. Mithöfer, A holistic approach to analyze systemic jasmonate accumulation in individual leaves of arabidopsis rosettes upon wounding, Front. Plant Sci. 871 (2018) 1–13, https://doi.org/10.3389/fpls.2018.01569.
L. Hoermayer, J.C. Montesinos, P. Marhava, E. Benková, S. Yoshida, J. Friml, Wounding-induced changes in cellular pressure and localized auxin signalling spatially coordinate restorative divisions in roots, Proc. Natl. Acad. Sci. U. S. A. 117 (2020) 15322–15331, https://doi.org/10.1073/pnas.2003346117.
S.C. Hoo, A.J.K. Koo, X. Gao, S. Jayanty, B. Thines, A.D. Jones, G.A. Howe, Regulation and function of arabidopsis JASMONATE ZIM-domain genes in response to wounding and herbivory, Plant Physiol. 146 (2008) 952–964, https://doi.org/10.1104/pp.107.115691.
K. Ichimura, T. Mizoguchi, R. Yoshida, T. Yuasa, K. Shinozaki, Various abiotic stresses rapidly activate Arabidopsis MAP kinases ATMPK4 and ATMPK6, Plant J. 24 (2000) 655–665, https://doi.org/10.1046/j.1365-313X.2000.00913.x.
K. Ichimura, K. Shinozaki, G. Tena, J. Sheen, Y. Henry, A. Champion, M. Kreis, S. Zhang, H. Hirt, C. Wilson, E. Heberle-Bors, B.E. Ellis, P.C. Morris, R.W. Innes, J.R. Ecker, D. Scheel, D.F. Klessig, Y. Machida, J. Mundy, Y. Ohashi, J.C. Walker, Mitogen-activated protein kinase cascades in plants: a new nomenclature, Trends Plant Sci. 7 (2002) 301–308, https://doi.org/10.1016/S1360-1385(02)02302-6.
L. Jiang, Y. Chen, L. Luo, S.C. Peck, Central roles and regulatory mechanisms of dual-specificity MAPK phosphatases in developmental and stress signaling, Front. Plant Sci. 871 (2018) 1–13, https://doi.org/10.3389/fpls.2018.01697.
P.K. Kandoth, S. Ranf, S.S. Pancholi, S. Jayanty, M.D. Walla, W. Miller, G.A. Howe, D. E. Lincoln, J.W. Stratmann, Tomato MAPKs LeMPK1, LeMPK2, and LeMPK3 function in the systemin-mediated defense response against herbivorous insects, Proc. Natl. Acad. Sci. 104 (2007) 12205–12210, https://doi.org/10.1073/pnas.0700344104.
S.D. Lawrence, M.B. Blackburn, J. Shao, N.G. Novak, The response to cabbage looper infestation in Arabidopsis is altered by lowering levels of Zat18 a Q-type C2H2 zinc finger protein, J. Plant Interact. 17 (2022) 198–205, https://doi.org/10.1080/17429145.2021.2024285.
R. Liu, Y. Liu, N. Ye, G. Zhu, M. Chen, L. Jia, Y. Xia, L. Shi, W. Jia, J. Zhang, AtDsPTP1 acts as a negative regulator in osmotic stress signalling during Arabidopsis seed germination and seedling establishment, J. Exp. Bot. 66 (2015) 1339–1353, https://doi.org/10.1093/jxb/eru484.
Y. Liu, S. Zhang, Phosphorylation of 1-aminocyclopropane-1-carboxylic acid synthase by MPK6, a stress-responsive mitogen-activated protein kinase, induces ethylene biosynthesis in Arabidopsis, Plant Cell 16 (2004) 3386–3399, https://doi.org/10.1105/tpc.104.026609.
C.J. Marshall, MAP kinase kinase kinase, MAP kinase kinase and MAP kinase, Curr. Opin. Genet. Dev. 4 (1994) 82–89, https://doi.org/10.1016/0959-437X(94)90095-7.
A. Mithöfer, G. Wanner, W. Boland, Effects of feeding Spodoptera littoralis on lima bean leaves. II. Continuous mechanical wounding resembling insect feeding is sufficient to elicit herbivory-related volatile emission, Plant Physiol. 137 (2005) 1160–1168, https://doi.org/10.1104/pp.104.054460.
M. Nomoto, M.J. Skelly, T. Itaya, T. Mori, T. Suzuki, T. Matsushita, M. Tokizawa, K. Kuwata, H. Mori, Y.Y. Yamamoto, T. Higashiyama, H. Tsukagoshi, S.H. Spoel, Y. Tada, Suppression of MYC transcription activators by the immune cofactor NPR1 fine-tunes plant immune responses, Cell Rep. 37 (2021), 110125, https://doi.org/10.1016/j.celrep.2021.110125.
V.K. Prajapati, M. Varma, J. Vadassery, In silico identification of effector proteins from generalist herbivore *Spodoptera litura*, BMC Genom. 21 (1) (2020) 16, https://doi.org/10.1186/s12864-020-07196-4.
N. Rayapuram, J. Bigeard, H. Alhoraibi, L. Bonhomme, A.M. Hesse, J. Vinh, H. Hirt, D. Pflieger, Quantitative phosphoproteomic analysis reveals shared and specific targets of Arabidopsis mitogen-activated protein kinases (MAPKs) MPK3, MPK4, and MPK6, Mol. Cell. Proteom. 17 (2018) 61–80, https://doi.org/10.1074/mcp.RA117.000135.
E.A. Schmelz, J. Engelberth, H.T. Alborn, J.H. Tumlinson, P.E.A. Teal, Phytohormone-based activity mapping of insect herbivore-produced elicitors, Proc. Natl. Acad. Sci. U. S. A. 106 (2009) 653–657, https://doi.org/10.1073/pnas.0811861106.
C.A. Schneider, W.S. Rasband, K.W. Eliceiri, NIH Image to ImageJ: 25 years of image analysis, Nat. Methods 9 (2012) 671–675, https://doi.org/10.1038/nmeth.2089.
A. Schweighofer, H. Hirt, I. Meskiene, Plant PP2C phosphatases: emerging functions in stress signaling, Trends Plant Sci. 9 (2004) 236–243, https://doi.org/10.1016/j.tplants.2004.03.007.
A. Schweighofer, V. Kazanaviciute, E. Scheikl, M. Teige, R. Doczi, H. Hirt, M. Schwanninger, M. Kant, R. Schuurink, F. Mauch, A. Buchala, F. Cardinale, I. Meskiene, The PP2C-type phosphatase AP2C1, which negatively regulates MPK4 and MPK6, modulates innate immunity, jasmonic acid, and ethylene levels in Arabidopsis, Plant Cell 19 (2007) 2213–2224, https://doi.org/10.1105/tpc.106.049585.
L.B. Sheard, X. Tan, H. Mao, J. Withers, G. Ben-Nissan, T.R. Hinds, Y. Kobayashi, F.-F. Hsu, M. Sharon, J. Browse, S.Y. He, J. Rizo, G. a Howe, N. Zheng, Jasmonate perception by inositol-phosphate-potentiated COI1-JAZ co-receptor, Nature 468 (2010) 400–405, https://doi.org/10.1038/nature09430.
C. Sözen, S.T. Schenk, M. Boudsocq, C. Chardin, M. Almeida-Trapp, A. Krapp, H. Hirt, A. Mithöfer, J. Colcombet, Wounding and insect feeding trigger two independent MAPK pathways with distinct regulation and kinetics, Plant Cell 32 (2020) 1988–2003, https://doi.org/10.1105/tpc.19.00917.
F.C. Sussmilch, T.J. Brodribb, S.A.M. McAdam, Up-regulation of NCED3 and ABA biosynthesis occur within minutes of a decrease in leaf turgor but AHK1 is not required, J. Exp. Bot. 68 (2017) 2913–2918, https://doi.org/10.1093/jxb/erx124.
F. Takahashi, R. Yoshida, K. Ichimura, T. Mizoguchi, S. Seo, M. Yonezawa, K. Maruyama, K. Yamaguchi-Shinozaki, K. Shinozakia, The mitogen-activated protein kinase cascade MKK3-MPK6 is an important part of the jasmonate signal transduction pathway in Arabidopsis, Plant Cell 19 (2007) 805–818, https://doi.org/10.1105/tpc.106.046581.
R. Ulm, K. Ichimura, T. Mizoguchi, S.C. Peck, T. Zhu, X. Wang, K. Shinozaki, J. Paszkowski, Distinct regulation of salinity and genotoxic stress responses by Arabidopsis MAP kinase phosphatase 1, EMBO J. 21 (2002) 6483–6493, https://doi.org/10.1093/emboj/cdf646.
J. Umbrasaite, A. Schweighofer, V. Kazanaviciute, Z. Magyar, Z. Ayatollahi, V. Unterwurzacher, C. Choopayak, J. Boniecka, J.A.H. Murray, L. Bogre, I. Meskiene, MAPK phosphatase AP2C3 induces ectopic proliferation of epidermal cells leading to stomata development in Arabidopsis, PLoS One 5 (2010), https://doi.org/10.1371/journal.pone.0015357.
D. Van der Does, A. Leon-Reyes, A. Koornneef, M.C. Van Verk, N. Rodenburg, L. Pauwels, A. Goossens, A.P. Körbes, J. Memelink, T. Ritsema, S.C.M. Van Wees, C.M. J. Pietersea, Salicylic acid suppresses jasmonic acid signaling downstream of SCFCOI1-JAZ by targeting GCC promoter motifs via transcription factor ORA59, Plant Cell 25 (2013) 744–761, https://doi.org/10.1105/tpc.112.108548.
M.C. van Verk, J.F. Bol, H.J.M. Linthorst, WRKY transcription factors involved in activation of SA biosynthesis genes, BMC Plant Biol. 11 (2011), 89, https://doi.org/10.1186/1471-2229-11-89.
A. Verhage, I. Vlaardingerbroek, C. Raaymakers, N.M. Van Dam, M. Dicke, S.C.M. Van Wees, C.M.J. Pieterse, Rewiring of the jasmonate signaling pathway in Arabidopsis during insect herbivory, Front. Plant Sci. 2 (2011) 1–12, https://doi.org/10.3389/fpls.2011.00047.
D. Verma, P.K. Bhagat, A.K. Sinha, MKK3-MPK6-MYC2 module positively regulates ABA biosynthesis and signalling in Arabidopsis, J. Plant Biochem. Biotechnol. 29 (2020) 785–795, https://doi.org/10.1007/s13562-020-00621-5.
I.A. Vos, A. Verhage, R.C. Schuurink, L.G. Watt, C.M.J. Pieterse, S.C.M. Van Wees, Onset of herbivore-induced resistance in systemic tissue primed for jasmonate-dependent defenses is activated by abscisic acid, Front. Plant Sci. 4 (2013) 1–10, https://doi.org/10.3389/fpls.2013.00539.
C. Wasternack, B. Hause, Jasmonates: biosynthesis, perception, signal transduction and action in plant stress response, growth and development. An update to the 2007 review in Annals of Botany, Ann. Bot. 111 (2013) 1021–1058, https://doi.org/10.1093/aob/mct067.
J. Wei, J.J.A. van Loon, R. Gols, T.R. Menzel, N. Li, L. Kang, M. Dicke, Reciprocal crosstalk between jasmonate and salicylate defence-signalling pathways modulates plant volatile emission and herbivore host-selection behaviour, J. Exp. Bot. 65 (2014) 3289–3298, https://doi.org/10.1093/jxb/eru181.
D. Winter, B. Vinegar, H. Nahal, R. Ammar, G.V. Wilson, N.J. Provart, An "electronic fluorescent pictograph" browser for exploring and analyzing large-scale biological data sets, PLoS One 2 (2007), https://doi.org/10.1371/journal.pone.0000718.
J. Wu, C. Hettenhausen, S. Meldau, I.T. Baldwin, Herbivory rapidly activates MAPK signaling in attacked and unattacked leaf regions but not between leaves of Nicotiana attenuata, Plant Cell 19 (2007) 1096–1122, https://doi.org/10.1105/tpc.106.049353.
Y. Xing, W. Jia, J. Zhang, AtMKK1 and AtMPK6 are involved in abscisic acid and sugar signaling in Arabidopsis seed germination, Plant Mol. Biol. 70 (2009) 725–736, https://doi.org/10.1007/s11103-009-9503-0.
X. Yan, S. Chen, Regulation of plant glucosinolate metabolism, Planta 226 (2007) 1343–1352, https://doi.org/10.1007/s00425-007-0627-7.

Q. Yu, X. Hua, H. Yao, Q. Zhang, J. He, L. Peng, D. Li, Y. Yang, X. Li, Abscisic acid receptors are involves in the Jasmonate signaling in Arabidopsis, Plant Signal. Behav. 16 (2021), https://doi.org/10.1080/15592324.2021.1948243.
L. Zhang, J. Yao, J. Withers, X.F. Xin, R. Banerjee, Q. Fariduddin, Y. Nakamura, K. Nomura, G.A. Howe, W. Boland, H. Yan, S.Y. He, Host target modification as a strategy to counter pathogen hijacking of the jasmonate hormone receptor, Proc. Natl. Acad. Sci. U. S. A. 112 (2015) 14354–14359, https://doi.org/10.1073/pnas.1510745112.
M. Zhang, S. Zhang, Mitogen-activated protein kinase cascades in plant signaling, J. Integr. Plant Biol. 64 (2022) 301–341, https://doi.org/10.1111/jipb.13215.
C. Zhao, H. Nie, Q. Shen, S. Zhang, W. Lukowitz, D. Tang, EDR1 physically interacts with MKK4/MKK5 and negatively regulates a MAP kinase cascade to modulate plant innate immunity, PLoS Genet. 10 (2014), https://doi.org/10.1371/journal.pgen.1004389.